doi:10.1093/brain/aws230 Brain 2012: 135; 3380–3391 | 3380

BRAIN
A JOURNAL OF NEUROLOGY

Molecular analysis and biochemical classification of TDP-43 proteinopathy

Hiroshi Tsuji,[1,2] Tetsuaki Arai,[3,4] Fuyuki Kametani,[1] Takashi Nonaka,[1] Makiko Yamashita,[1] Masami Suzukake,[1] Masato Hosokawa,[3] Mari Yoshida,[5] Hiroyuki Hatsuta,[6] Masaki Takao,[6] Yuko Saito,[7] Shigeo Murayama,[6] Haruhiko Akiyama,[3] Masato Hasegawa,[1] David M. A. Mann[8] and Akira Tamaoka[2]

1 Department of Neuropathology and Cell Biology, Tokyo Metropolitan Institute of Medical Science, Tokyo 156-8585, Japan
2 Department of Neurology, Graduate School of Comprehensive Human Sciences, University of Tsukuba, Tsukuba-shi 305-8576, Japan
3 Department of Dementia and Higher Brain Function, Tokyo Metropolitan Institute of Medical Science, Tokyo 156-8585, Japan
4 Department of Psychiatry, Graduate School of Comprehensive Human Sciences, University of Tsukuba, Tsukuba-shi 305-8576, Japan
5 Department of Neuropathology, Institute for Medical Science of Aging, Aichi Medical University, Aichi 480-1195, Japan
6 Department of Neuropathology, Tokyo Metropolitan Institute of Gerontology, Tokyo 173-0015, Japan
7 Department of Pathology and Laboratory Medicine, National Center Hospital of Neurology and Psychiatry, Tokyo 187-8551, Japan
8 Mental Health and Neurodegeneration Research Group, Greater Manchester Neuroscience Centre, University of Manchester, Manchester M13 9PT, UK

Correspondence to: Masato Hasegawa,
Department of Neuropathology and Cell Biology,
Tokyo Metropolitan Institute of Medical Science,
2-1-6 Kamikitazawa,
Setagaya-ku,
Tokyo 156-8506,
Japan
E-mail: hasegawa-ms@igakuken.or.jp

Amyotrophic lateral sclerosis and frontotemporal lobar degeneration with TAR DNA-binding protein of 43 kDa pathology are progressive neurodegenerative diseases that are characterized by intracytoplasmic aggregates of hyperphosphorylated TAR DNA-binding protein of 43 kDa. These TAR DNA-binding protein 43 proteinopathies can be classified into subtypes, which are closely correlated with clinicopathological phenotypes, although the differences in the molecular species of TAR DNA-binding protein 43 in these diseases and the biological significance thereof, remain to be clarified. Here, we have shown that although the banding patterns of abnormally phosphorylated C-terminal fragments of TAR DNA-binding protein 43 differ between the neuropathological subtypes, these are indistinguishable between multiple brain regions and spinal cord in individual patients. Immunoblot analysis of protease-resistant TAR DNA-binding protein 43 demonstrated that the fragment patterns represent different conformations of TAR DNA-binding protein 43 molecular species in the diseases. These results suggest a new clinicopathological classification of TAR DNA-binding protein 43 proteinopathies based on their molecular properties.

Keywords: amyotrophic lateral sclerosis; frontotemporal lobar degeneration; TDP-43; classification

Abbreviations: ALS = amyotrophic lateral sclerosis; FTLD = frontotemporal lobar degeneration; FTLD-TDP = frontotemporal lobar degeneration with TAR DNA-binding protein of 43 kDa pathology; TDP-43 = TAR DNA-binding protein of 43 kDa

Received March 13, 2012. Revised June 3, 2012. Accepted June 28, 2012. Advance Access publication October 3, 2012

Introduction

Amyotrophic lateral sclerosis (ALS) and frontotemporal lobar degeneration with TDP-43 pathology (FTLD-TDP) are sporadic and familial neurodegenerative diseases characterized neuropathologically by intracytoplasmic aggregates of TAR DNA-binding protein of 43 kDa (TDP-43) (Arai *et al.*, 2006; Neumann *et al.*, 2006). In ALS, upper and lower motor neurons progressively degenerate. Neuropathologically, the TDP-43-positive structures appear as rounded or skein-like inclusions in the lower motor neurons. Similar TDP-43-positive inclusions are also observed in the prefrontal gyrus that contains the upper motor neurons. Moreover, TDP-43-positive glial cytoplasmic inclusions are found close to the upper and lower motor neurons in ALS (Tan *et al.*, 2007). In FTLD-TDP, TDP-43 pathology is distinguished into four histological subtypes (types A–D) based on the predominant type of TDP-43-positive structures present (Mackenzie *et al.*, 2011). Type A is characterized by numerous short dystrophic neurites and crescentic or oval neuronal cytoplasmic inclusions; type B has moderate numbers of neuronal cytoplasmic inclusions, throughout all cortical layers, but few dystrophic neurites; type C has a predominance of elongated dystrophic neurites in upper cortical layers, with few neuronal cytoplasmic inclusions; and type D refers to the pathology associated with inclusion body myopathy with early onset Paget disease and frontotemporal dementia caused by *VCP* mutations, characterized by numerous short dystrophic neurites and frequent lentiform neuronal intranuclear inclusions. There is a relationship between subtypes of TDP-43 pathology and clinical phenotype, and many cases of ALS and frontotemporal lobar degeneration (FTLD) are readily distinguished by each clinical symptom. However, some cases have symptoms of both ALS and FTLD. ALS with dementia refers to cases initially presenting with motor neuron disease becoming demented, whereas FTLD-motor neuron disease refers to cases presenting with cognitive impairment and subsequently developing motor neuron disease.

TDP-43 pathology is also present in a subset of familial ALS and FTLD due to mutations in *TARDBP* (Kabashi *et al.*, 2008; Sreedharan *et al.*, 2008), progranulin (*GRN*; Baker *et al.*, 2006) and *C9ORF72* (DeJesus-Hernandez *et al.*, 2011; Renton *et al.*, 2011) genes. Although most patients with mutations in *TARDBP* present with ALS, some present with FTLD (Gitcho *et al.*, 2009; Kovacs *et al.*, 2009). Cases with FTLD-TDP with *GRN* mutation often show type A pathology (Mackenzie *et al.*, 2006b; Cairns *et al.*, 2007b; Josephs *et al.*, 2007). The pathology of ALS and FTLD due to mutations in *C9ORF72* is heterogeneous: TDP-43 pathology overlaps between ALS and FTLD-TDP types A and B (Murray *et al.*, 2011). One large multicentre study of sporadic and familial FTLD-TDP showed broad overlap between the TDP-43 subtyping, especially between types A and B (Armstrong *et al.*, 2010). These overlaps might occur because current pathological classification may be inadequate, as it is based solely on the morphological assessment of certain subjective cortical regions. A more objective and unbiased classification is needed.

In this study, we have investigated a wide range of patients with various TDP-43 proteinopathies to investigate whether patterns of protease-resistant TDP-43 might indicate different TDP-43 strain types, and characterize the TDP-43 C-terminal banding patterns in multiple regions of the CNS, basing our approach on the method used for demonstration of prion strain variation and the aetiology of new variant Creutzfeldt–Jakob disease (Collinge *et al.*, 1996). We show at least three C-terminal banding patterns that distinguish diseases with TDP-43 proteinopathy and report that the banding pattern in individual patients is indistinguishable in different brain regions and spinal cord. Corresponding patterns of protease-resistant phosphorylated TDP-43 are also seen between the pathological phenotypes. As with the prion diseases, the present results suggest that the different conformation of abnormal TDP-43 deposits in the CNS in patients corresponding with various subtypes of TDP-43 proteinopathy, and that the conformation state of the abnormal TDP-43 protein may determine the pathological phenotype.

Materials and methods

Patients

Human brain tissues were obtained from the Brain Donation Programme at the University of Tsukuba (Japan), Tokyo Metropolitan Institute of Gerontology (Japan), National Shimofusa Mental Hospital (Japan) and the University of Manchester (UK). This study was approved by the local Research Ethics Committee. The subjects in this study included eight patients with ALS, five patients with FTLD-TDP type A, eight patients with FTLD-TDP type B, six patients with FTLD-TDP type C and two patients with Alzheimer's disease without TDP-43 pathology. All cases with ALS met the revised El Escorial criteria for ALS (Brooks, 1994) without dementia. All cases with FTLD-TDP fulfilled clinical diagnostic criteria of FTLD (Neary *et al.*, 1998), and classifications of TDP-43 subtype were made in accordance with published guidelines (Cairns *et al.*, 2007*a*; Mackenzie *et al.*, 2011). Four patients with FTLD-TDP type A were cases of familial FTLD-U with *GRN* mutations. One familial ALS case, one with type A, and two with type B had the GGGCC repeat expansion in *C9ORF72*. The age, gender, brain regions examined and clinical diagnosis are given in Table 1.

A fresh frozen tissue sample was taken and cut into two pieces. One piece was fixed in 4% paraformaldehyde in 0.1 M phosphate buffer (pH 7.4) for 2 days and was used for immunohistochemical analysis. The other piece was homogenized and used for immunoblot analysis. In principle, we took the precentral gyrus and lumbar part of the spinal cord in the ALS cases, and the frontal lobe in the FTLD-TDP cases, because TDP-43 pathology is always known to be prevalent in these regions (Tan *et al.*, 2007; Geser *et al.*, 2008, 2009). However, the spinal cord was not available in four cases with ALS, and both motor regions in two cases were not available. In these cases, the frontal lobe was examined instead. For ALS Cases 1, 3, 5 and ALS and FTLD-TDP type C Case 22, the whole of the cerebral hemisphere and brainstem were available as fresh frozen tissues. In these four cases, we took the multiple regions, as described in Table 1. Every tissue sample was examined immunohistochemically for TDP-43-positive lesions. All samples, except some from the cerebellar cortex, showed an accumulation of abnormal TDP-43-positive structures.

Immunoblotting

Sarkosyl-insoluble, urea-soluble fractions were extracted from each region as previously described (Arai *et al.*, 2006; Hasegawa *et al.*, 2008).

Table 1 **Description of the patients**

Case number	Age at death (year)	Age at onset (year)	Sex	Family history	Brain weight (g)	Clinical diagnosis	Region
ALS							
1	62	61	M	N	1150	ALS	Prec, L and other regions[a]
2	72	71	F	N	1390	ALS	Prec and L
3	42	40	F	N	1140	ALS	Prec, L and other regions[a]
4	76	75	F	N	NA	ALS	Prec and L
5	62	54	M	N	1230	ALS	Prec and other regions[a]
6	77	76	F	N	NA	ALS	Prec
7	67	65	M	N	1414	ALS	Fr
8	55	53	M	Y(m*C9ORF72*)	1250	ALS	Fr
FTLD-TDP type A							
9	58	49	M	Y(m*C9ORF72*)	1050	FTD	Fr
10	67	54	F	Y(m*GRN*)	NA	FTD	Fr
11	71	63	F	Y(m*GRN*)	863	PNFA	Fr
12	66	56	F	Y(m*GRN*)	1100	FTD	Fr
13	68	60	M	Y(m*GRN*)	1210	FTD + MND	Fr
FTLD-TDP type B							
14	45	43	M	N	1260	FTD + MND	Fr
15	59	57	M	Y(m*C9ORF72*)	1210	FTD + MND	Fr
16	67	65	M	N	1280	FTD + MND	Fr
17	76	74	M	N	1215	FTD + MND	Fr
18	69	58	M	N	1166	FTD + MND	Fr
19	52	50	F	Y(m*C9ORF72*)	1050	FTD + MND	Fr
20	65	61	M	N	1530	FTD + MND	Fr
21	68	64	M	N	1213	FTD + MND	Fr
FTLD-TDP type C							
22	82	NA	M	N	1200	SD	Fr, Te and other regions[b]
23	67	65	M	N	NA	SD	Fr
24	59	53	M	N	NA	SD	Fr
25	63	58	M	N	NA	SD	Fr
26	66	55	F	N	1035	SD	Fr
27	75	60	M	N	1174	SD	Fr
AD							
28	65	56	F	N	1165	AD	Fr
29	70	NA	F	N	1126	AD	Fr

AD = Alzheimer's disease; Fr = frontal cortex; FTD = frontotemporal dementia; L = lumbar part of spinal cord; m*C9ORF72* = mutation of chromosome 9 open-reading frame 72 gene; m*GRN* = mutation of progranulin gene; MND = motor neuron disease; NA = not available; PNFA = progressive non-fluent aphasia; Prec = precentral gyrus; SD = semantic dementia; Y = yes; N = no.

a Other regions contained striatum, thalamus, hippocampus dentate gyrus, substantia nigra, pons, medulla and cerebellum cortex. In these cases, the grey and white matter of precentral gyrus were separated from each other macroscopically and examined.

b Other regions contain striatum, thalamus, hippocampus dentate gyrus, substantia nigra, pons, medulla and cerebellum cortex. FTLD-TDP type B without MND and type D are not analysed in this study.

The samples were loaded on 15% SDS–PAGE gels. Proteins in the gel were then transferred onto a polyvinylidene difluoride membrane (Millipore). After blocking with 3% gelatine in 0.01 M PBS (pH 7.4), membranes were incubated overnight with phosphorylation dependent anti-TDP-43 rabbit polyclonal antibody (pS409/410, 1:1000; Hasegawa *et al.*, 2008), phosphorylation independent TDP-43 polyclonal antibody 10782-1-AP (TDP-43 pAb, 1:3000) and TDP-43 monoclonal antibody, 60019-2-Ig (TDP-43 mAb, 1:3000) (ProteinTech Group). After incubation with the appropriate biotinylated secondary antibody, immunolabelling was detected using the VECTASTAIN® ABC system (Vector Laboratories) coupled with a 3,3′-diaminobenzidine reaction intensified with nickel chloride. The blot membranes were digitally analysed, and densitometric analyses were performed with ImageJ version 1.44p (NIH, http://rsbweb.nih.gov/ij/index.html). The densitometry data were averaged for all cases in each group to illustrate the different patterns.

Immunohistochemistry

After cryoprotection in 15% sucrose in 0.01 M PBS (pH 7.4), paraformaldehyde-fixed tissue blocks were cut on a freezing microtome at 30-μm thickness. The free-floating sections were immunostained with phosphorylation-dependent TDP-43 monoclonal antibody (pS409/410, 1:10 000) (Inukai *et al.*, 2008) for 72 h in the cold. After treatment with mouse secondary antibody, immunolabelling was detected using the VECTASTAIN ®ABC system coupled with a 3,3′-diaminobenzidine reaction to yield a brown precipitate. Sections were lightly counterstained with heamatoxylin.

Protease treatment of phosphorylated TDP-43

Sarkosyl-insoluble fractions extracted from the neocortical regions of patients with ALS or FTLD-TDP were treated with final concentration of 100 μg/ml trypsin (Promega) or 10 μg/ml chymotrypsin (Sigma-Aldrich) at 37°C for 30 min. The reaction was stopped by boiling for 5 min. After centrifuging at 15 000 rpm for 1 min, the samples were analysed by immunoblotting as described earlier.

Mass spectrometry

Sarkosyl-insoluble, trypsin-resistant fractions were loaded on 15% SDS–PAGE gels. The pS409/410-positive ~16 kDa bands were dissected and digested in-gel with chymotrypsin. The digests were applied to the Paradigm MS4 high-performance liquid chromatography system (Microm BioResources). A reversed phase capillary column (Develosil ODS-HG5, 0.075 × 150 mm, Nomura Chemical) was used at a flow rate of 300 nl/min with a 4–80% linear gradient of acetonitrile in 0.1% formic acid. Eluted peptides were directly detected with an ion trap mass spectrometer, LXQ (Thermo Fisher Scientific). The obtained spectra were analysed with Mascot (Matrix Science).

Statistical analysis

The *P*-values for the description of the statistical significance of differences were calculated by means of the paired, two-tailed *t*-test using Prism 5.04 software (GraphPad Software, Inc).

Results

Banding patterns of phosphorylated C-terminal TDP-43 in ALS and FTLD with TDP-43 pathology

Immunoblot analysis using an antibody specific for abnormal TDP-43, pS409/410, showed high-molecular-weight smearing substances, phosphorylated full-length TDP-43 at 45 kDa and several C-terminal fragments at 18–26 kDa to be present in affected brain regions in all cases (Fig. 1). Three major bands at 23, 24 and 26 kDa, and two minor bands at 18 and 19 kDa were seen in the precentral gyrus and frontal cortex of cases with ALS, with the 24 kDa band being the most intense (Fig. 1A and F). In the lumbar spinal cord, the two minor bands at 18 and 19 kDa were barely present, but the banding pattern of the three major bands at 23, 24 and 26 kDa was similar to that in the cerebral cortex (Fig. 1A). No such pS409/410-positive TDP-43 bands were detected in control cases with Alzheimer's disease with no TDP-43 pathology (Fig. 1B). In the FTLD-TDP cases, the banding pattern could be distinguished into three types according to the FTLD-TDP histological subtype (Fig. 1C–E). In FTLD-TDP type A, three major bands at 23, 24 and 26 kDa, and two minor bands at 18 and 19 kDa were detected, with the 23 kDa band being the most intense (Fig. 1C and F). In FTLD-type B cases, the banding pattern was the same as that in the ALS cases (Fig. 1D and F). In FTLD-TDP type C cases, two major bands at 23 and 24 kDa, and two minor bands at 18 and 19 kDa were detected, with the 24 kDa band being the most intense, and the band at 26 kDa being hardly detectable (Fig. 1E and F). Densitometric analyses of the immunoblots for all cases are shown in Supplementary Fig. 1. Each component of the C-terminal fragments was significantly different (Fig. 1F).

Immunoblot analysis using phosphorylation independent TDP-43 polyclonal and monoclonal antibodies detected phosphorylated full-length TDP-43 at 45 kDa, two bands ~25 kDa and high-molecular-weight smears, in addition to the normal TDP-43 band at 43 kDa in ALS and various subtypes of FTLD-TDP. The banding patterns between ALS and various subtypes of FTLD-TDP could not be distinguished with these antibodies. In the cases with Alzheimer's disease, the normal TDP-43 band at 43 kDa was detected, but neither the phosphorylated 45 kDa band nor the ~25 kDa fragments were observed (Supplementary Fig. 2). Immunoblot analysis of α-tubulin in Tris saline-soluble fractions from cases with types A, B and C pathology showed no correlation between the banding pattern of α-tubulin and that of TDP-43 (Supplementary Fig. 3), indicating that the differences in the banding patterns are not because of protein degradation caused by a long post-mortem interval or unfavourable agonal status.

Immunohistochemistry and immunoblot analyses of phosphorylated TDP-43 in multiple regions of ALS and FTLD with TDP-43 pathology

In ALS cases, the neuronal cytoplasmic pathology, which included skein-like inclusions, irregularly shaped TDP-immunoreactive neuronal cytoplasmic inclusions and densely staining granules, was confirmed in multiple regions by immunohistochemistry analysis using pS409/410 (Fig. 2A–G). Glial cytoplasmic inclusions were also present in many regions. Glial cytoplasmic inclusions were more frequent in the white matter than in the grey matter (Fig. 2H). A few neuronal cytoplasmic inclusions were found in the cerebellar cortex granule cells (Fig. 2G). In FTLD-TDP type C, dystrophic neurites were seen in multiple regions except for the cerebellar cortex (Fig. 2I–O), whereas neuronal cytoplasmic inclusions were also present in the striatum and hippocampus dentate gyrus granule cells (Fig. 2J and L). No abnormal structures were found in the cerebellar cortex (data not shown). These observations show that pathological TDP-43 is present throughout many CNS areas in ALS, suggesting that ALS does not selectively affect only the motor system, but it is rather a multisystem neurodegenerative TDP-43 proteinopathy.

Immunoblot analyses of three ALS cases confirmed that phosphorylated TDP-43 and the C-terminal fragments are deposited in multiple brain regions in ALS (Fig. 3A). Relatively strong immunoreactivities were detected in the striatum (in Cases 3 and 5) and substantia nigra (in Cases 1 and 5), although this varied between cases (Fig. 3A). Importantly, the banding pattern for the TDP-43 C-terminal fragments in these three cases was basically the same in all brain regions examined (Fig. 3A). In FTLD-TDP type C, a C-terminal banding pattern, clearly distinct from that

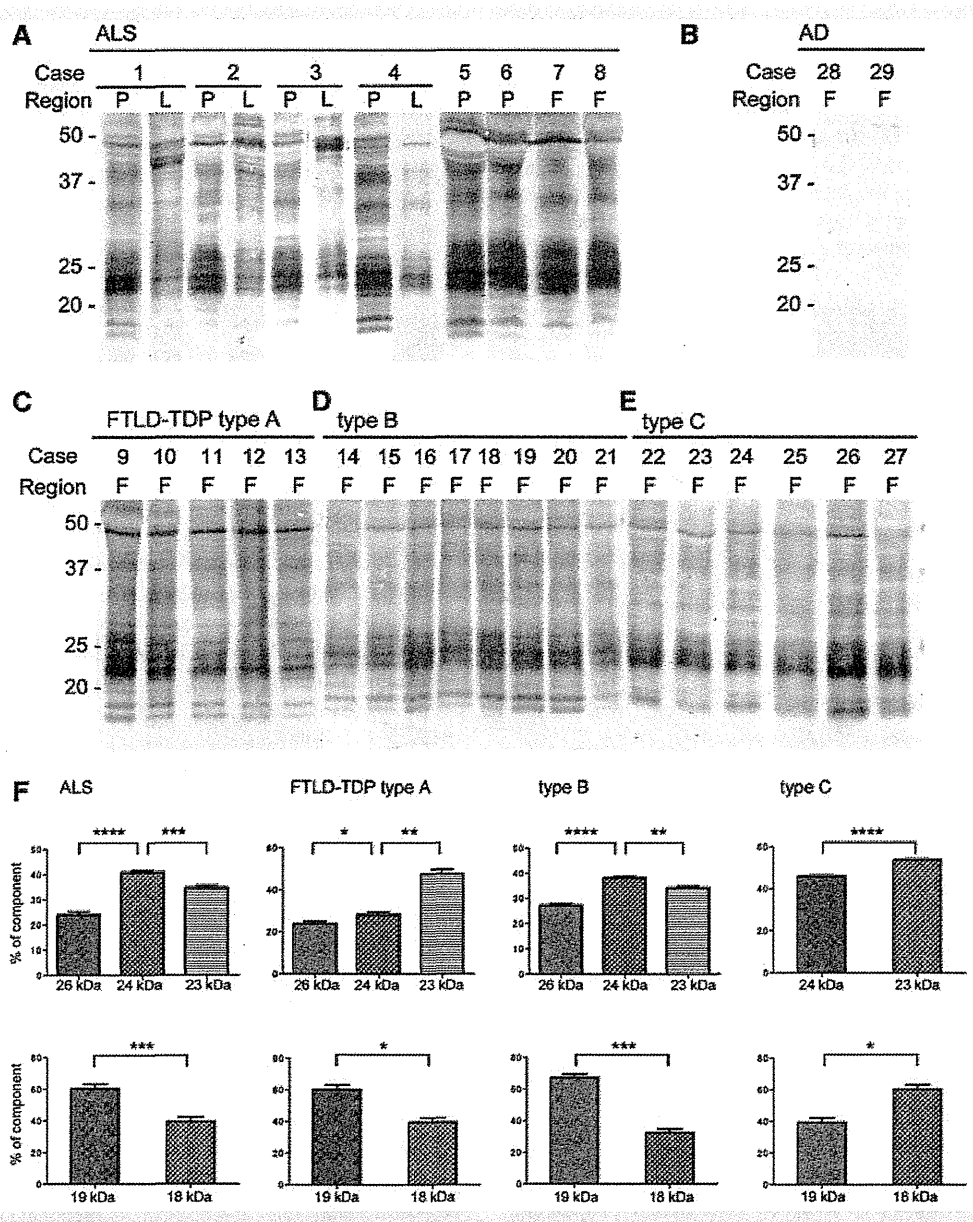

Figure 1 Immunoblot analyses of sarkosyl-insoluble TDP-43 in the brains or spinal cords of ALS (Cases 1–8) (**A**), Alzheimer's disease (Cases 28–29) (**B**), FTLD-TDP type A (Cases 9–13) (**C**), FTLD-TDP type B (Cases 14–21) (**D**) and FTLD-TDP type C (Cases 22–27) (**E**), using a phosphorylation-dependent anti-TDP-43 antibody (pS409/410). In all cases, high-molecular-weight smearing substances, phosphorylated full-length TDP-43 at 45 kDa and several C-terminal fragments at 18–26 kDa are detected. In ALS (**A**) and FTLD-TDP type B (**D**) cases, three major bands at 23, 24 and 26 kDa and two minor bands at 18 and 19 kDa are detected, whereas in the FTLD-TDP Type C (**E**) cases, two major bands at 23 and 24 and two minor bands at 18 and 19 kDa. A 24 kDa band is the most intense in ALS (**A**) and FTLD-TDP type B (**E**), whereas a 23 kDa band is the most intense in FTLD-TDP type C (**D**). The band pattern of the cases with type A (**C**) is an intermediate between FTLD-TDP type B (**D**) and FTLD-TDP type C (**E**). In spinal cords of cases with ALS, the 18 and 19 kDa bands are hardly detectable, but the same banding pattern of the 23–26 kDa bands as in precentral gyrus is detected. No such TDP-43 fragments are detected in brains of patients with Alzheimer's disease (AD) (**B**). The intensity of each C-terminal band was analysed using the ImageJ software and each component was statistically analysed by Student's *t*-test (**F**). Data indicate mean (SEM). $^{****}P < 0.0001$, $^{***}P < 0.001$, $^{**}P < 0.01$, $^{*}P < 0.05$. F = frontal cortex; L = lumbar part of spinal cord; P = precentral cortex.

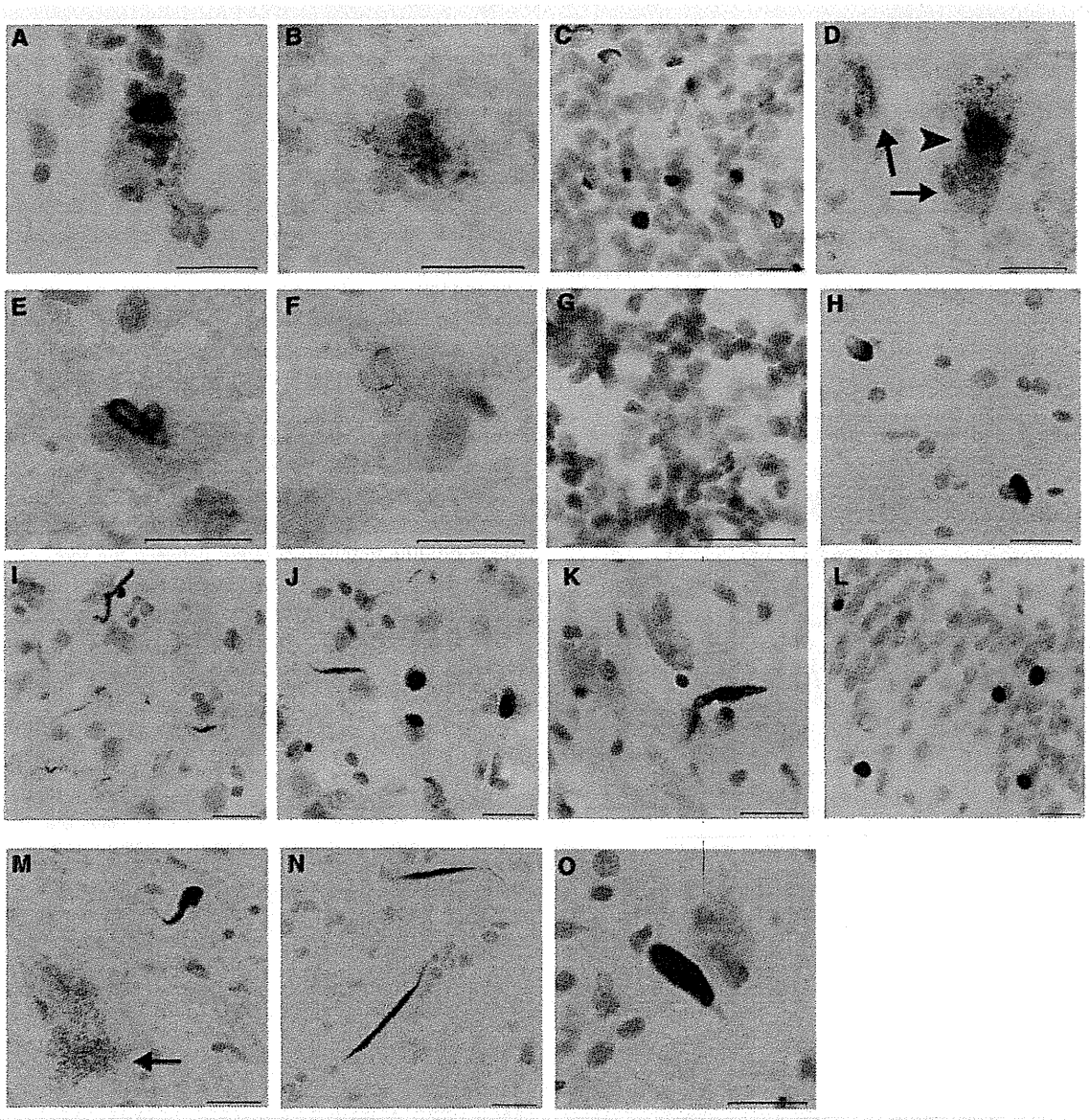

Figure 2 Phosphorylated TDP-43-positive structures observed in different brain regions and spinal cords of ALS (**A–H**) and FTLD-type C (**I–O**) using a phosphorylation-dependent anti-TDP-43 antibody (pS409/410). (**A**) Lewy body-like inclusion in the striatum neuron. (**B**) Cytoplasmic granular staining in the thalamus. (**C**) Neuronal cytoplasmic inclusions in the granular cells of hippocampus. (**D**) Irregularly shaped TDP-immunoreactive neuronal cytoplasmic inclusion in the substantia nigra (arrowhead). The arrows denote neuromelanin granules. (**E**) Skein-like inclusion in the motor nucleus of trigeminal nerve of pons. (**F**) Skein-like inclusion in the inferior olivary nucleus of medulla. (**G**) Neuronal cytoplasmic inclusion in the granular cells of cerebellar cortex. (**H**) Glial cytoplasmic inclusions in the white matter of precentral cortex. (**I**) Dystrophic neurites in the temporal cortex, (**J**) dystrophic neurites and neuronal cytoplasmic inclusions in the striatum. (**K**) Dystrophic neurites in the thalamus. (**L**) Neuronal cytoplasmic inclusions in the granular cells of hippocampus. (**M**) Dystrophic neurites in the substantia nigra. The arrow denotes neuromelanin granules. (**N**) Dystrophic neurites in the pons. (**O**) Dystrophic neurites in the medullary reticular formation. Scale bars = 20 μm.

of ALS, was detected in the temporal cortex, striatum and hippocampus, but was barely detected in the thalamus, substantia nigra, pons and medulla, and not at all in the cerebellar cortex (Fig. 3B). The banding pattern observed in these brain regions was indistinguishable (Fig. 3B). These results suggest that the same abnormal TDP-43 molecular species is deposited in different brain regions and different cell types, although the morphology of the TDP-43 inclusions may be different in the brain regions. Densitometric analyses of the immunoblots for all cases are shown in Supplementary Fig. 4.

Protease-resistant TDP-43 in ALS and FTLD with frontotemporal dementia-43 pathology

These different banding patterns in TDP-43 proteinopathies may represent different conformations of abnormal TDP-43 or their aggregates. To test this hypothesis, we subjected the abnormal TDP-43 recovered in the sarkosyl-insoluble pellets to protease treatment and analysed the protease-resistant bands. Proteins can be easily cleaved by proteases if they are denatured or unstructured, but domains that have rigid structures, such as a β-sheet conformation or that are structurally buried or interacting with other molecules, are highly resistant to proteases. On trypsin or chymotrypsin treatment, the full-length 45-kDa band and the smearing substance of TDP-43 disappeared, leaving protease-resistant fragments at 16–25 kDa (Figs 4 and 5). As expected, the protease-resistant banding patterns were different and distinguishable into three patterns (Figs 4 and 5). In ALS, trypsin-resistant doublet bands at 16 and 15 kDa, and two minor bands at ~24 kDa were detected, whereas a single band at 16 kDa and some additional bands at ~24 kDa were detected in FTLD-TDP type A (Fig. 4A, Lanes 1 and 2). In FTLD-TDP type B, the same banding pattern as that in ALS was observed (Fig. 4A, Lane 3). In FTLD-TDP type C, a broad single band at 16 kDa and some additional bands at ~24 kDa were detected (Fig. 4A, Lane 4). No such bands were detected in Alzheimer's disease (Fig. 4A, Lane 5).

Similarly, on chymotrypsin treatment, multiple protease-resistant bands were detected at 16–25 kDa and the chymotrypsin-resistant band patterns were also different between the three disease subtypes (Fig. 4B). Doublet bands were seen in ALS and FTLD-TDP type B, but only a single band in FTLD-TDP type C was detected at ~16 kDa (Fig. 4B). In FTLD-TDP type A, the lower band (15 kDa) of the ~16 kDa doublet was more intense than the upper one (16 kDa).

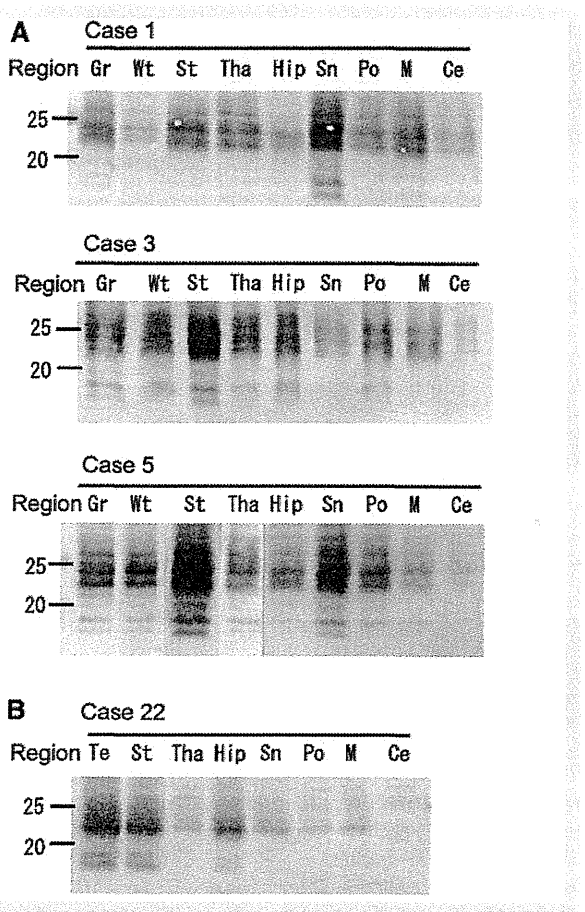

Figure 3 Immunoblot analyses of the C-terminal fragments of phosphorylated TDP-43 in the different brain regions of cases with ALS (Cases 1, 3 and 5, as shown in Fig. 1) **(A)** and FTLD-type C (Case 22, as shown in Fig. 1) **(B)**. **(A)** Immunoblots of insoluble TDP-43 in the grey or white matter of precentral cortex, striatum, thalamus, hippocampus, substantia nigra, pons and medulla of ALS cases. **(B)** Immunoblot of TDP-43 in temporal cortex, striatum, hippocampus, thalamus, substantia nigra, pons and cerebellar cortex of the case with FTLD-TDP type C. Ce = Cerebellar cortex; Gr = grey matter of precentral gyrus; Hip = hippocampus; M = medulla; Po = pons; Sn = substantia nigra; St = striatum; Tha = thalamus; Te = temporal cortex; Wt = white matter of precentral gyrus. Immunoblots of spinal cords of cases with ALS are shown in Fig. 1.

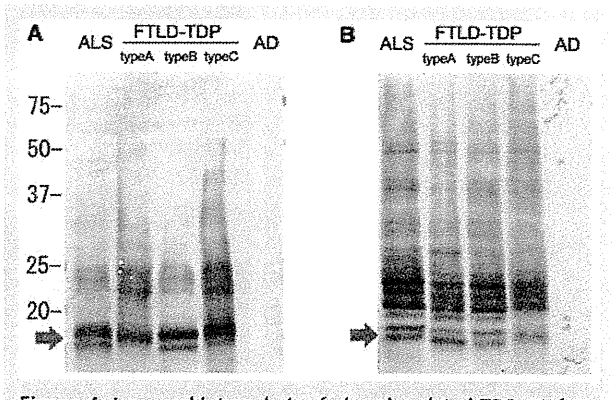

Figure 4 Immunoblot analysis of phosphorylated TDP-43 from representative ALS and FTLD-TDP cases after protease treatment. **(A)** Immunoblot of insoluble TDP-43 from cases with ALS, FTLD-TDP type A, type B, type C and Alzheimer's disease (AD) after trypsin treatment. Doublet bands at ~16 kDa (arrow) and some minor 23–24 kDa bands are detected in ALS and FTLD-TDP type B, whereas a single band at ~16 kDa and several bands at 23 and 24 kDa are detected in FTLD-TDP type A and type C. No such bands are detected in the Alzheimer's disease case. **(B)** Immunoblot of insoluble TDP-43 from cases with ALS, FTLD-TDP type A, type B, type C and Alzheimer's disease after chymotrypsin treatment. Multiple protease-resistant TDP-43 bands are detected at 16–25 kDa. Doublet bands at ~16 kD (arrow) are detected in ALS and FTLD-TDP type A and B, whereas a single band at ~16 kD (arrow) is detected in the case with FTLD-TDP type C. In FTLD-TDP type A, the lower band of the doublet at 16 kDa is more intense. No such bands are detected in the Alzheimer's disease case.

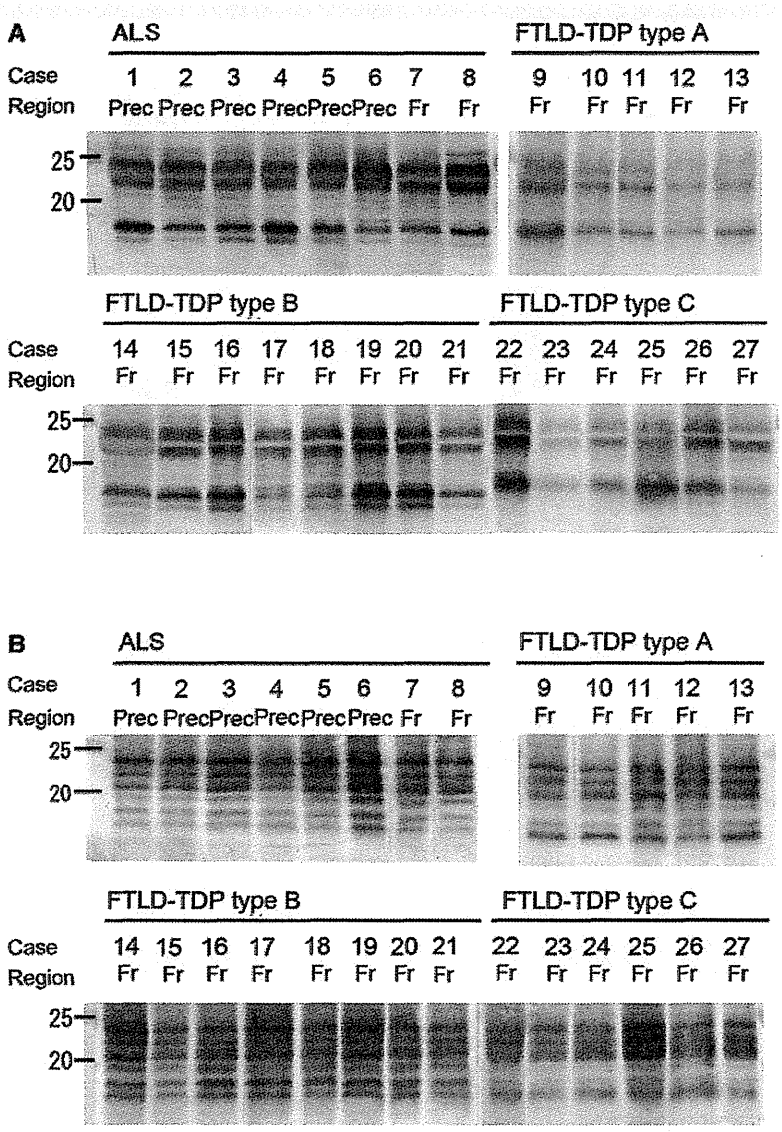

Figure 5 Comparison of the protease-resistant TDP-43 banding patterns in ALS and FTLD-TDP. Immunoblot analyses of trypsin-resistant (**A**) and chymotrypsin-resistant (**B**) fragments of TDP-43 from all cases examined. The banding patterns of ALS and FTLD-TDP type B cases are indistinguishable. Fr = frontal cortex; Prec = precentral gyrus.

In all cases examined, the trypsin-resistant banding patterns were clearly distinguishable between the disease subtypes in accordance with the three different types of banding pattern of TDP-43 C-terminal fragments, although it is difficult to distinguish the trypsin band pattern of type A from that of type C (Figs 5A, 6A and Supplementary Fig. 5). The chymotrypsin-resistant banding patterns were distinguishable and could be differentiated into three types (Figs 5B, 6B and Supplementary Fig. 6), also in accordance with the banding pattern of the TDP-43 C-terminal fragment. The banding patterns of ALS and FTLD-TDP type B were the same, whereas the banding pattern of FTLD-TDP type A was distinguishable from those of type C and type B (Figs 4 and 5). The combination analyses of trypsin and chymotrypsin-resistant banding patterns confirmed that TDP-43 proteinopathies can also be biochemically distinguishable into three types according to TDP-43 subtypes. These results strongly suggest that the different C-terminal banding patterns represent different conformations of TDP-43 aggregates and that the distinct types of TDP-43 are deposited in association with distinct pathological phenotypes of TDP-43 proteinopathies.

Immunoblot analysis using phosphorylation independent TDP-43 polyclonal and monoclonal antibodies detected some TDP-43 fragments in the ALS and FTLD-TDP cases after trypsin or chymotrypsin treatment, although no clear difference was observed in the banding patterns between ALS and other subtypes of FTLD-TDP (Supplementary Fig. 7). The distinctive

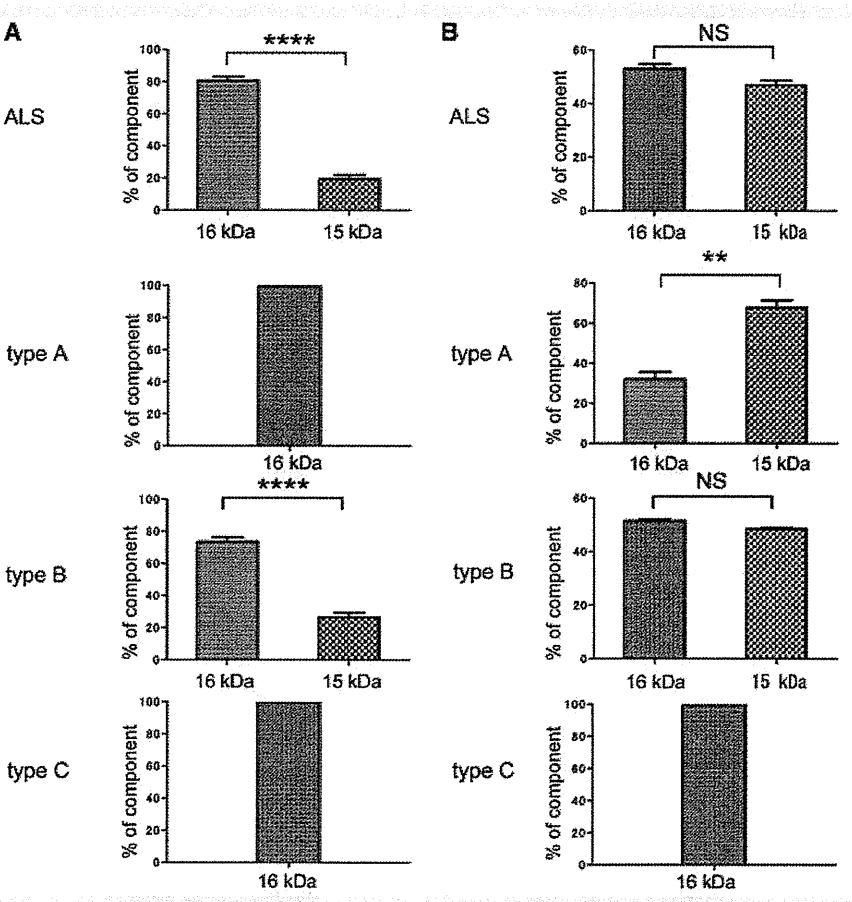

Figure 6 Quantitative analysis of protease-resistant ~16 kDa band. **(A)** The intensity of trypsin-resistant ~16 kDa band of each case was quantitated with ImageJ and statistically analysed. **(B)** The intensity of chymotrypsin-resistant ~16 kDa band of each case was quantitated with ImageJ and statistically analysed. Data indicate mean (SEM). $****P < 0.0001$, $**P < 0.01$, NS = not significant.

protease-resistant bands at ~16 kDa of ALS were not detected with both phosphorylation independent antibodies (Supplementary Fig. 8).

We also analysed the banding pattern of phosphorylated TDP-43 in another series of five sporadic cases with TDP-43 pathology (Alzheimer's disease, Alzheimer's disease/dementia with Lewy bodies and Alzheimer's disease/argyrophilic grain disease) (Supplementary Table 1). The banding pattern of the C-terminal fragments, and trypsin- or chymotrypsin-resistant fragments, in these were same as those of FTLD-TDP type A with *GRN* mutation (Supplementary Fig. 9).

Mass spectrometric analysis of protease-resistant bands of TDP-43 in ALS and FTLD-TDP type C

To further investigate the differences in the abnormal TDP-43 protein species at a molecular level, we analysed the ~16 kDa trypsin-resistant bands by mass spectrometry. Mass analysis of chymotrypsin digests of ~16 kDa trypsin-resistant fragments identified 4 peptides, amino acid residues 277–289, 290–299, 294–333 and 300–316, suggesting these peptides are derived from trypsin-resistant fragments 276–414 and 294–414. Mass spectrometric analysis of the single broad band from FTLD-TDP type C identified the peptides of amino acids 273–283, 277–289, 290–313 and 317–330, strongly suggesting that the trypsin-resistant fragments from FTLD-TDP type C are derived from peptides 273–414 and 276–414. These analyses clearly indicate that trypsin-resistant core regions of the abnormal TDP-43 accumulated in the brain are not necessarily the same between ALS and FTLD (Supplementary Fig. 10).

Discussion

In this study, we have shown that the banding patterns for TDP-43 C-terminal fragments in ALS and FTLD are distinguishable and classifiable into at least three types. This difference was consistently demonstrated in 27 cases, eight with ALS, five with FTLD-TDP type A, eight with FTLD-TDP type B and six with FTLD-TDP type C. These results strongly suggest that distinct

types of TDP-43 molecules constitute the distinct types of pathologies of TDP-43 and determine the clinicopathological phenotypes of TDP-43 proteinopathies. In TDP-43 histopathology, ALS is considered to represent a distinct pathological subtype because the distribution of TDP-43 inclusions is different from that of FTLD-TDP (Mackenzie *et al.*, 2006a). However, as shown in this study, the TDP-43 accumulations in ALS and FTLD-TDP type B are biochemically indistinguishable. In fact, clinical and histopathological motor neuron disease is often present in cases with FTLD-TDP type B histology. In the three types of phosphorylated C-terminal TDP-43 banding pattern, the pattern seen in FTLD-TDP type C is the most distinctive, lacking the 26 kDa band detected in ALS, FTLD-TDP type A and type B cases (Fig. 1). The clinical diagnosis of the FTLD-TDP type C cases was semantic dementia in every instance, consistent with other studies showing this type of histology to be associated with semantic dementia (Mackenzie *et al.*, 2006a). FTLD is clinically classified into frontotemporal dementia, demantic dementia and progressive non-fluent aphasia, based on topographical distributions of degeneration (Neary *et al.*, 1998). In frontotemporal dementia, the bilateral frontal and temporal lobes are affected, whereas the bilateral temporal lobes are affected in semantic dementia and the left hemisphere in progressive non-fluent aphasia. Present data showing the most distinctive pattern of abnormal TDP-43 in type C indicate that semantic dementia may be biochemically different from frontotemporal dementia. Similar differences in tau fragment banding patterns have been shown between progressive supranuclear palsy and corticobasal degeneration (Arai *et al.*, 2004). Progressive supranuclear palsy and corticobasal degeneration are neurodegenerative diseases that are characterized by intracytoplasmic aggregates of hyperphosphorylated tau with four microtubule-binding repeats, with distinctive pathological features. Immunoblot analysis of Sarkosyl-insoluble tau demonstrated that a 33 kDa C-terminal fragment of tau band predominated in progressive supranuclear palsy, whereas two closely related bands of ~37 kDa predominated in corticobasal degeneration. The clinicopathological subtypes of these diseases may be explained by different conformations of protein aggregates or species of abnormal proteins.

Unfortunately, we were unable to obtain brain tissue samples from patients with FTLD-TDP type D (associated with *VCP* mutation; Cairns *et al.*, 2007b; Neumann *et al.*, 2007). However, because the deposition of abnormal TDP-43 in this disorder is mostly within neuronal nuclei, it is possible that the conformation of abnormal TDP-43 in FTLD-TDP type D may also differ from that in FTLD-TDP types A–C. Familial ALS and FTLD-TDP cases in which known mutations [*GRN* (Baker *et al.*, 2006) or *C9ORF72* (DeJesus-Hernandez *et al.*, 2011; Renton *et al.*, 2011)] were examined in this study. In FTLD-TDP due to *GRN* mutations, type A pathology is exclusively seen (Mackenzie *et al.*, 2006b; Cairns *et al.*, 2007b; Josephs *et al.*, 2007). All our cases with FTLD with *GRN* mutation showed the same C-terminal banding patterns of phosphorylated TDP-43 corresponding to type A histology. Some recent studies describing the clinical and pathological features of cases of FTLD-TDP with hexanucleotide repeat expansions in *C9ORF72* reported that many of the 'pure' frontotemporal dementia cases had type A pathology, whereas many of the combined frontotemporal dementia and motor neuron disease cases had type B pathology (Murray *et al.*, 2011; Boeve *et al.*, 2012; Hsiung *et al.*, 2012; Mahoney *et al.*, 2012; Simon-Sanchez *et al.*, 2012; Snowden *et al.*, 2012). Present cases with *C9ORF72* expansions included one case of ALS, one case of pure frontotemporal dementia with type A pathology, and two cases of frontotemporal dementia with motor neuron disease and type B pathology. The C-terminal banding pattern of these cases with familial ALS and frontotemporal dementia with motor neuron disease was not different from that in the sporadic ALS and FTLD-TDP type B cases, and that of the frontotemporal dementia case was not different from that in the cases with *GRN* mutation. Therefore, expansions in *C9ORF72* do not seem to influence the various types of TDP-43 C-terminal banding pattern or histological type of TDP-43 pathology.

Immunohistochemical studies using TDP-43 antibodies have shown that pathological TDP-43 is present throughout many CNS areas in ALS, suggesting that ALS does not selectively affect only the motor system, but is rather a multisystem neurodegenerative TDP-43 proteinopathy (Geser *et al.*, 2008). We also confirmed this viewpoint, immunohistochemically and biochemically, finding the same disease characteristic C-terminal fragment (banding) patterns of phosphorylated TDP-43 within the cerebral cortex, spinal cord and the other different brain regions in ALS. Although the types of pathological structures or their morphologies detected on immunohistochemistry analysis appeared different, the banding patterns for the C-terminal fragments were the same in all regions examined in three patients with ALS. This was also true for the one case with FTLD-TDP type C, where the same banding pattern of the C-terminal fragments was detected in several different brain regions beyond the frontal cortex (Fig. 3). These results strongly suggest that the same abnormal TDP-43 molecule is deposited in different brain regions in ALS (and probably also in FTLD-TDP type B) and FTLD-TDP type C, although we need to examine whether this is also true for cases with FTLD-TDP type A. Importantly, the extent of the abnormal protein pathology is closely correlated with the disease progression, such as Alzheimer's disease in tauopathies (Braak and Braak, 1991), and Parkinson's disease in α-synucleinopathies (Braak *et al.*, 2003; Saito *et al.*, 2003). However, the molecular mechanisms governing different clinicopathological phenotypes of these neurodegenerative diseases and their progression are poorly understood. Recent studies using cellular or animal models have suggested that aggregation-prone proteins, such as tau and α-synuclein, can spread to other cells and brain regions like prion disorders (Clavaguera *et al.*, 2009; Frost *et al.*, 2009; Nonaka *et al.*, 2010). The spreading of α-synuclein lesions to the grafts is also observed in Parkinson's disease brains after transplantation (Li *et al.*, 2008). However, it remains to be clarified whether the 'propagating' abnormal protein species represents a distinct 'strain type' that can be differentiated by molecular criteria in human patients or whether the species are the same in different brain regions.

We have also shown that the banding patterns of protease-resistant fragments of phosphorylated TDP-43 are similarly different in accordance with the banding patterns seen in untreated C-terminal fragments, confirming the direct link between neuropathological subtypes and biochemical banding patterns. The mass spectrometric analysis indicated that the protease resistant regions

of abnormal TDP-43 are different between the diseases. As abnormally phosphorylated TDP-43 has been shown to accumulate in a filamentous form in ALS spinal cords (Hasegawa *et al.*, 2008), the filament core regions may be different between the diseases. Protease-resistant bands, and differences in banding patterns, have been reported in the prion diseases, Creutzfeldt–Jakob disease and bovine spongiform encephalopathy (Collinge *et al.*, 1996). Protease-resistant prion protein extracted from cases with new-variant Creutzfeldt–Jakob disease showed a different and characteristic pattern from that in cases with sporadic Creutzfeldt–Jakob disease, with the banding pattern being indistinguishable from that of mice infected with bovine spongiform encephalopathy prion. Protease-treated prion protein species are thought to have different mobilities because of different conformations. These observations in prion disease suggest that the different banding patterns to the abnormal TDP-43 fragments in ALS and FTLD might represent different TDP-43 strains with different conformations.

Recently, TDP-43 pathology has been detected in some cases with Alzheimer's disease (Arai *et al.*, 2009). We have shown here that the banding patterns of TDP-43 in cases of Alzheimer's disease with TDP-43 pathology are the same as those in FTLD-TDP type A. These novel observations suggest a biochemical commonality between FTLD and Alzheimer's disease with respect to TDP-43 pathology.

The results shown in this study also suggest a molecular basis for the clinicopathological classification of TDP-43 proteinopathies, which complements the histological classifications (Mackenzie *et al.*, 2011).

Funding

This work was supported by a Grant-in-Aid for Scientific Research (A) (to M.H., 11000624) from Ministry of Education, Culture, Sports, Science and Technology of Japan, and grants from Ministry of Health, Labor and Welfare of Japan (to M.H.).

Supplementary material

Supplementary material is available at *Brain* online.

References

Arai T, Mackenzie IR, Hasegawa M, Nonoka T, Niizato K, Tsuchiya K, et al. Phosphorylated TDP-43 in Alzheimer's disease and dementia with Lewy bodies. Acta Neuropathol (Berl) 2009; 117: 125–36.

Arai T, Hasegawa M, Akiyama H, Ikeda K, Nonaka T, Mori H, et al. TDP-43 is a component of ubiquitin-positive tau-negative inclusions in frontotemporal lobar degeneration and amyotrophic lateral sclerosis. Biochem Biophys Res Commun 2006; 351: 602–11.

Arai T, Ikeda K, Akiyama H, Nonaka T, Hasegawa M, Ishiguro K, et al. Identification of amino-terminally cleaved tau fragments that distinguish progressive supranuclear palsy from corticobasal degeneration. Ann Neurol 2004; 55: 72–9.

Armstrong RA, Ellis W, Hamilton RL, Mackenzie IR, Hedreen J, Gearing M, et al. Neuropathological heterogeneity in frontotemporal lobar degeneration with TDP-43 proteinopathy: a quantitative study of 94 cases using principal components analysis. J Neural Transm 2010; 117: 227–39.

Baker M, Mackenzie IR, Pickering-Brown SM, Gass J, Rademakers R, Lindholm C, et al. Mutations in progranulin cause tau-negative frontotemporal dementia linked to chromosome 17. Nature 2006; 442: 916–19.

Boeve BF, Boylan KB, Graff-Radford NR, Dejesus-Hernandez M, Knopman DS, Pedraza O, et al. Characterization of frontotemporal dementia and/or amyotrophic lateral sclerosis associated with the GGGGCC repeat expansion in *C9ORF72*. Brain 2012; 135: 765–83.

Braak H, Braak E. Neuropathological stageing of Alzheimer-related changes. Acta Neuropathol 1991; 82: 239–59.

Braak H, Del Tredici K, Rub U, de Vos RA, Jansen Steur EN, Braak E. Staging of brain pathology related to sporadic Parkinson's disease. Neurobiol Aging 2003; 24: 197–211.

Brooks BR. El Escorial World Federation of Neurology criteria for the diagnosis of amyotrophic lateral sclerosis. Subcommittee on Motor Neuron Diseases/Amyotrophic Lateral Sclerosis of the World Federation of Neurology Research Group on Neuromuscular Diseases and the El Escorial "Clinical limits of amyotrophic lateral sclerosis" workshop contributors. J Neurol Sci 1994; 124 (Suppl): 96–107.

Cairns NJ, Bigio EH, Mackenzie IR, Neumann M, Lee VM, Hatanpaa KJ, et al. Neuropathologic diagnostic and nosologic criteria for frontotemporal lobar degeneration: consensus of the Consortium for Frontotemporal Lobar Degeneration. Acta Neuropathol 2007a; 114: 5–22.

Cairns NJ, Neumann M, Bigio EH, Holm IE, Troost D, Hatanpaa KJ, et al. TDP-43 in familial and sporadic frontotemporal lobar degeneration with ubiquitin inclusions. Am J Pathol 2007b; 171: 227–40.

Clavaguera F, Bolmont T, Crowther RA, Abramowski D, Frank S, Probst A, et al. Transmission and spreading of tauopathy in transgenic mouse brain. Nat Cell Biol 2009; 11: 909–13.

Collinge J, Sidle KC, Meads J, Ironside J, Hill AF. Molecular analysis of prion strain variation and the aetiology of 'new variant' CJD. Nature 1996; 383: 685–90.

DeJesus-Hernandez M, Mackenzie IR, Boeve BF, Boxer AL, Baker M, Rutherford NJ, et al. Expanded GGGGCC hexanucleotide repeat in noncoding region of *C9ORF72* causes chromosome 9p-linked FTD and ALS. Neuron 2011; 72: 245–56.

Frost B, Jacks RL, Diamond MI. Propagation of tau misfolding from the outside to the inside of a cell. J Biol Chem 2009; 284: 12845–52.

Geser F, Brandmeir NJ, Kwong LK, Martinez-Lage M, Elman L, McCluskey L, et al. Evidence of multisystem disorder in whole-brain map of pathological TDP-43 in amyotrophic lateral sclerosis. Arch Neurol 2008; 65: 636–41.

Geser F, Martinez-Lage M, Robinson J, Uryu K, Neumann M, Brandmeir NJ, et al. Clinical and pathological continuum of multisystem TDP-43 proteinopathies. Arch Neurol 2009; 66: 180–9.

Gitcho MA, Bigio EH, Mishra M, Johnson N, Weintraub S, Mesulam M, et al. TARDBP 3'-UTR variant in autopsy-confirmed frontotemporal lobar degeneration with TDP-43 proteinopathy. Acta Neuropathol 2009; 118: 633–45.

Hasegawa M, Arai T, Nonaka T, Kametani F, Yoshida M, Hashizume Y, et al. Phosphorylated TDP-43 in frontotemporal lobar degeneration and amyotrophic lateral sclerosis. Ann Neurol 2008; 64: 60–70.

Hsiung GY, Dejesus-Hernandez M, Feldman HH, Sengdy P, Bouchard-Kerr P, Dwosh E, et al. Clinical and pathological features of familial frontotemporal dementia caused by *C9ORF72* mutation on chromosome 9p. Brain 2012; 135: 709–22.

Inukai Y, Nonaka T, Arai T, Yoshida M, Hashizume Y, Beach TG, et al. Abnormal phosphorylation of Ser409/410 of TDP-43 in FTLD-U and ALS. FEBS Lett 2008; 582: 2899–904.

Josephs KA, Ahmed Z, Katsuse O, Parisi JF, Boeve BF, Knopman DS, et al. Neuropathologic features of frontotemporal lobar degeneration with ubiquitin-positive inclusions with progranulin gene (*GRN*) mutations. J Neuropathol Exp Neurol 2007; 66: 142–51.

Kabashi E, Valdmanis PN, Dion P, Spiegelman D, McConkey BJ, Vande Velde C, et al. TARDBP mutations in individuals with sporadic and familial amyotrophic lateral sclerosis. Nat Genet 2008; 40: 572–4.

Kovacs GG, Murrell JR, Horvath S, Haraszti L, Majtenyi K, Molnar MJ, et al. TARDBP variation associated with frontotemporal dementia, supranuclear gaze palsy, and chorea. Mov Disord 2009; 24: 1843–7.

Li JY, Englund E, Holton JL, Soulet D, Hagell P, Lees AJ, et al. Lewy bodies in grafted neurons in subjects with Parkinson's disease suggest host-to-graft disease propagation. Nat Med 2008; 14: 501–3.

Mackenzie IR, Baborie A, Pickering-Brown S, Du Plessis D, Jaros E, Perry RH, et al. Heterogeneity of ubiquitin pathology in frontotemporal lobar degeneration: classification and relation to clinical phenotype. Acta Neuropathol 2006a; 112: 539–49.

Mackenzie IR, Baker M, Pickering-Brown S, Hsiung GY, Lindholm C, Dwosh E, et al. The neuropathology of frontotemporal lobar degeneration caused by mutations in the progranulin gene. Brain 2006b; 129: 3081–90.

Mackenzie IR, Neumann M, Baborie A, Sampathu DM, Du Plessis D, Jaros E, et al. A harmonized classification system for FTLD-TDP pathology. Acta Neuropathol 2011; 122: 111–13.

Mahoney CJ, Beck J, Rohrer JD, Lashley T, Mok K, Shakespeare T, et al. Frontotemporal dementia with the *C9ORF72* hexanucleotide repeat expansion: clinical, neuroanatomical and neuropathological features. Brain 2012; 135: 736–50.

Murray ME, DeJesus-Hernandez M, Rutherford NJ, Baker M, Duara R, Graff-Radford NR, et al. Clinical and neuropathologic heterogeneity of c9FTD/ALS associated with hexanucleotide repeat expansion in *C9ORF72*. Acta Neuropathol 2011; 122: 673–90.

Neary D, Snowden JS, Gustafson L, Passant U, Stuss D, Black S, et al. Frontotemporal lobar degeneration: a consensus on clinical diagnostic criteria. Neurology 1998; 51: 1546–54.

Neumann M, Mackenzie IR, Cairns NJ, Boyer PJ, Markesbery WR, Smith CD, et al. TDP-43 in the ubiquitin pathology of frontotemporal dementia with *VCP* gene mutations. J Neuropathol Exp Neurol 2007; 66: 152–7.

Neumann M, Sampathu DM, Kwong LK, Truax AC, Micsenyi MC, Chou TT, et al. Ubiquitinated TDP-43 in frontotemporal lobar degeneration and amyotrophic lateral sclerosis. Science 2006; 314: 130–3.

Nonaka T, Watanabe ST, Iwatsubo T, Hasegawa M. Seeded aggregation and toxicity of α-synuclein and tau: cellular models of neurodegenerative diseases. J Biol Chem 2010; 285: 34885–98.

Renton AE, Majounie E, Waite A, Simon-Sanchez J, Rollinson S, Gibbs JR, et al. A hexanucleotide repeat expansion in *C9ORF72* is the cause of chromosome 9p21-linked ALS-FTD. Neuron 2011; 72: 257–68.

Saito Y, Kawashima A, Ruberu NN, Fujiwara H, Koyama S, Sawabe M, et al. Accumulation of phosphorylated alpha-synuclein in aging human brain. J Neuropathol Exp Neurol 2003; 62: 644–54.

Simon-Sanchez J, Dopper EG, Cohn-Hokke PE, Hukema RK, Nicolaou N, Seelaar H, et al. The clinical and pathological phenotype of *C9ORF72* hexanucleotide repeat expansions. Brain 2012; 135: 723–35.

Snowden JS, Rollinson S, Thompson JC, Harris JM, Stopford CL, Richardson AM, et al. Distinct clinical and pathological characteristics of frontotemporal dementia associated with *C9ORF72* mutations. Brain 2012; 135: 693–708.

Sreedharan J, Blair IP, Tripathi VB, Hu X, Vance C, Rogelj B, et al. TDP-43 mutations in familial and sporadic amyotrophic lateral sclerosis. Science 2008; 319: 1668–72.

Tan CF, Eguchi H, Tagawa A, Onodera O, Iwasaki T, Tsujino A, et al. TDP-43 immunoreactivity in neuronal inclusions in familial amyotrophic lateral sclerosis with or without SOD1 gene mutation. Acta Neuropathol 2007; 113: 535–42.

NEUROPATHOLOGY

Neuropathology 2012; **32**, 595–603 doi:10.1111/j.1440-1789.2012.01302.x

Original Article

Reduced brain-derived neurotrophic factor (BDNF) mRNA expression and presence of BDNF-immunoreactive granules in the spinocerebellar ataxia type 6 (SCA6) cerebellum

Makoto Takahashi,[1] Kinya Ishikawa,[1] Nozomu Sato,[1] Masato Obayashi,[1] Yusuke Niimi,[1] Taro Ishiguro,[1] Mitsunori Yamada,[4,5] Yasuko Toyoshima,[4] Hitoshi Takahashi,[4] Takeo Kato,[6] Masaki Takao,[7,*] Shigeo Murayama,[3] Osamu Mori,[8] Yoshinobu Eishi[2] and Hidehiro Mizusawa[1]

Departments of [1]Neurology and Neurological Science and [2]Pathology, Graduate School, Tokyo Medical and Dental University, [3]Department of Neuropathology (The Brain Bank for Aging Research), Tokyo Metropolitan Geriatric Hospital and Institute of Gerontology, Tokyo, [4]Department of Pathology, Pathological Neuroscience Branch, Brain Research Institute, Niigata University, [5]Department of Clinical Research, National Hospital Organization, Saigata National Hospital, Niigata, [6]Department of Neurology, Hematology, Metabolism, Endocrinology and Diabetology (DNHMED), Yamagata University Faculty of Medicine, Yamagata, [7]Department of Neurology, Institute of Brain and Blood Vessels, Mihara Memorial Hospital, Gunma, and [8]Department of Internal Medicine and Neurology, Hatsuishi Hospital, Chiba, Japan

Spinocerebellar ataxia type 6 (SCA6) is an autosomal-dominant neurodegenerative disorder caused by a small expansion of tri-nucleotide (CAG) repeat encoding polyglutamine (polyQ) in the gene for α_{1A} voltage-dependent calcium channel ($Ca_v2.1$). Thus, this disease is one of the nine neurodegenerative disorders called polyQ diseases. The Purkinje cell predominant neuronal loss is the characteristic neuropathology of SCA6, and a 75-kDa carboxy-terminal fragment (CTF) of $Ca_v2.1$ containing polyQ, which remains soluble in normal brains, becomes insoluble in the cytoplasm of SCA6 Purkinje cells. Because the suppression of the brain-derived neurotrophic factor (BDNF) expression is a potentially momentous phenomenon in many other polyQ diseases, we implemented BDNF expression analysis in SCA6 human cerebellum using quantitative RT-PCR for the *BDNF* mRNA, and by immunohistochemistry for the BDNF protein. We observed significantly reduced *BDNF* mRNA levels in SCA6 cerebellum ($n = 3$) compared to controls ($n = 6$) (Mann–Whitney *U*-test, $P = 0.0201$). On immunohistochemistry, BDNF protein was only weakly stained in control cerebellum. On the other hand, we found numerous BDNF-immunoreactive granules in dendrites of SCA6 Purkinje cells. We did not observe similar BDNF-immunoreactive granules in other polyQ diseases, such as Huntington's disease or SCA2. As we often observed that the 1C2-positive $Ca_v2.1$ aggregates existed more proximally than the BDNF-positive granules in the dendrites, we speculated that the BDNF protein trafficking in dendrites may be disturbed by $Ca_v2.1$ aggregates in SCA6 Purkinje cells. We conclude that the SCA6 pathogenic mechanism associates with the *BDNF* mRNA expression reduction and abnormal localization of BDNF protein.

Key words: brain–derived neurotrophic factor (BDNF), immunohistochemistry, Purkinje cell, quantitative reverse transcription PCR (qRT-PCR), spinocerebellar ataxia type 6 (SCA6).

Correspondence: Kinya Ishikawa, MD, PhD, Department of Neurology and Neurological Science, Graduate School, Tokyo Medical and Dental University, 1-5-45, Yushima, Bunkyo-ku, Tokyo 113-8510, Japan. Email: pico.nuro@tmd.ac.jp

*Present address: Department of Neuropathology (The Brain Bank for Aging Research), Tokyo Metropolitan Geriatric Hospital and Institute of Gerontology, 35-2, Sakaecho, Itabashi-ku, Tokyo 173-0015, Japan.

Received 22 December 2011; revised 19 January 2012 and accepted 20 January 2012; published online 7 March 2012.

INTRODUCTION

Spinocerebellar ataxia type 6 (SCA6) is an autosomal-dominant neurodegenerative disorder clinically characterized by progressive cerebellar ataxia and gaze-evoked nystagmus with an average age of onset at 45.5 years.[1,2] The disease is caused by an expansion of the tri-nucleotide (CAG) repeat encoding polyglutamine (polyQ) in the gene for the α_{1A} (P/Q-type) voltage-dependent calcium channel protein ($Ca_v2.1$).[3] Thus, SCA6 is one of the polyQ diseases which consist of nine inherited neurological disorders caused by an expansion of the polyQ tract in the causative protein. The polyQ expansion causing SCA6 exists in the cytoplasmic carboxyl(C)-tail of the $Ca_v2.1$.[3] The Purkinje cell of the cerebellar cortex, which expresses $Ca_v2.1$ most abundantly in the brain, undergoes predominant degeneration.[2,4] Although it is not clear how the polyQ expansion in $Ca_v2.1$ causes the disease, $Ca_v2.1$ aggregation specifically observed in the SCA6 Purkinje cells is likely to harbor a clue.[4,5]

SCA6 has some unique features distinct from other polyQ diseases. First, the length of the polyQ tract expansion responsible for SCA6 is remarkably short and falls within the normal range of repeats for other polyQ diseases. The lengths of CAG repeats/polyQ tract are 20–33 repeats in SCA6 patients,[6,7] while they are required to be larger than 35 repeats for being causative in other polyQ diseases such as Huntington's disease (HD).[8] Second, microscopic $Ca_v2.1$ aggregates can be seen mainly in the cytoplasm (the cell body and cell processes) of SCA6 Purkinje cells, whereas in other polyQ diseases, aggregates with expanded polyQ are prevalent in the nuclei rather than in the cytoplasm of neurons expressing the responsible proteins.[9,10] These could indicate that the pathophysiology underlying SCA6 is quite different form that of other polyQ diseases.

The brain-derived neurotrophic factor (BDNF) is a multifunctional trophic factor expressed broadly in the CNS.[11] On the other hand, the brains affected with other polyQ diseases show a reduction in the BDNF gene expression. For example, the caudate nucleus and putamen of HD brains show reduced BDNF gene expression.[12] One of the possible mechanisms underlying this reduction is the sequestration of the cyclic-AMP responsive element binding protein (CREB)-binding protein (CBP) by the expanded polyQ in the neuronal nuclei, leading to the suppression of the CREB transcription, resulting in the reduction of BDNF transcription.[13] There may be another mechanism in HD. The wild-type huntingtin activates BDNF transcription in cultured CNS neurons by a pathway independent of CREB. However, the mutated huntingtin with expanded polyQ does not activate this pathway,[14] resulting in reduced BDNF transcription. Interestingly, overexpression of the BDNF in the striatum mitigates symptoms of HD in mice,[15] suggesting that the reduction of BDNF may be a substrate for therapy of polyQ diseases.

From these backgrounds, we carried out quantitative reverse transcription PCR (qRT-PCR) analysis to assess *BDNF* mRNA expression levels, and immunohistochemistry for investigating BDNF protein localization, both to see whether expression of BDNF is also altered in SCA6 cerebellum. Given that the reduced *BDNF* mRNA expression is determined by the sequestration of CBP in affected neuronal nuclei,[16–18] SCA6 brains may not show BDNF reduction, since nuclear $Ca_v2.1$ aggregates are very few in SCA6. However, we found that *BDNF* mRNA is also suppressed in SCA6 cerebellum. Interestingly, we also found that the BDNF protein forms definable granules in the SCA6 Purkinje cell dendrites. Here, we show that BDNF expression is abnormal in SCA6 human cerebellum.

MATERIALS AND METHODS

Specimens

Brain specimens obtained at autopsy with family consent were investigated. For assessing mRNA levels by qRT-PCR, three SCA6 and six control cerebellar tissues were examined (Table 1). These six controls were from individuals without obvious neurological diseases obtained from the Research Network of Aging Brain Research, Tokyo Metropolitan Geriatric Hospital and Institute of Gerontology. For immunohistochemistry, we studied five SCA6 patients, nine controls including three HD, one for each SCA2, SCA3/Machado-Joseph disease (MJD), dentatorubral and pallidoluysian atrophy (DRPLA), one Parkinson's disease, and two SCA31 patients (Table 1). The brains were fixed in formalin, and tissue sections were embedded in paraffin. Six-micron-thick sections were used for staining.

The study was approved by the institutional review boards of ethics of Tokyo Medical and Dental University and Tokyo Metropolitan Geriatric Hospital and Institute of Gerontology, and conformed to the tenets of the Declaration of Helsinki.

RNA extraction and qRT-PCR

Human brain tissues of the cerebellar hemispheric cortices, kept frozen at –80°C after autopsy, were dissected. Total RNA was isolated from each individual by TRIzol (Invitrogen, Carlsbad, CA, USA) and RNeasy mini kit (Qiagen, Valencia, CA, USA) according to the manufacturer's protocol. Then the total RNA was treated with DNase (Invitrogen) and quantified on a nanodrop spectrophotometer (Thermo Scientific, Wilmington, DE, USA). Reverse tran-

Table 1 Profiles of the investigated patients

Diagnosis	Individual no.	Age at death (years)/gender	Repeat size	Investigations
SCA6				
SCA6	Pt. 1	75/female	13/22	qRT-PCR, IHC
SCA6	Pt. 2	76/female	13/22	qRT-PCR, IHC
SCA6	Pt. 3	66/male	15/22	qRT-PCR, IHC
SCA6	Pt. 4	79/female	13/22	IHC
SCA6	Pt. 5	68/female	13/22	IHC
Controls				
Non-neurological	Ct. 1	57/male	Not examined	qRT-PCR
Non-neurological	Ct. 2	57/male	Not examined	qRT-PCR
Non-neurological	Ct. 3	62/male	Not examined	qRT-PCR
Non-neurological	Ct. 4	62/male	Not examined	qRT-PCR
Non-neurological	Ct. 5	90/male	Not examined	qRT-PCR
Non-neurological	Ct. 6	92/male	Not examined	qRT-PCR
Huntington's disease	Ct. 7	48/female	Not examined	IHC
Huntington's disease	Ct. 8	52/male	Not examined	IHC
Huntington's disease	Ct. 9	72/female	Not examined	IHC
SCA2	Ct.10	67/male	Not examined	IHC
Machado-Joseph disease	Ct.11	65/male	Not examined	IHC
Dentatorubral & pallidoluysian atrophy	Ct.12	58/female	Not examined	IHC
Parkinson's disease	Ct.13	88/male	Not examined	IHC
SCA31	Ct.14	74/male	11/13.	IHC
SCA31	Ct.15	79/male	11/14.	IHC

IHC, immunohistochemistry; qRT-PCR, quantitative reverse-transcription polymerase chain reaction.

scription generating complementary DNA (cDNA) was carried out with random hexmers and deoxy-thymidine oligomers (oligo-dT) mixtures using a PrimeScript™ RT Master Mix (TaKaRa Bio, Tokyo, Japan). The *BDNF* and glyceraldehyde-3-phophate degydrogenase (*GAPDH*) mRNA TaqMan® Gene Expression Assays ([BDNF] = Hs00380947 = m1, [GAPDH] = 4333764T) (Applied Biosystems, Foster City, CA, USA) were purchased, and qRT-PCR was performed by LightCycler 480II (Roche, Basel, Switzerland). The *BDNF* mRNA levels were calculated against the *GAPDH* mRNA expression levels in each sample.

The *BDNF* mRNA/*GAPDH* mRNA expression ratios were calculated using the delta-delta threshold cycle (Ct) method, and were compared between controls and SCA6 group. A standard *BDNF* mRNA/*GAPDH* mRNA ratio in one control subject was expressed as 1 (standard caliber) while the rest of the samples were presented with relative values to this standard. Each experiment was repeated three times independently and was averaged (mean ± SD). Finally, the controls ($n = 6$) and SCA6 ($n = 3$) groups were compared using Mann–Whitney *U*-test.

Immunohistochemistry of human brain tissues

Immunohistochemistry was carried out as described previously.[4,5,19] For antigen retrieval, tissue blocks were boiled by exposing microwaves three times for 1 min in 10 mmol citrate buffer (pH 7.4), rinsed in distilled water and then immersed in folic acid for 5 min. Sections were incubated overnight at 4°C with one of the following three antibodies: anti-BDNF antibody (rabbit polyclonal, sc546 [alternatively named N-20],[12] diluted at 1:100 with PBS ph7.4) (Santa Cruz Biotechnology, Santa Cruz, CA, USA), 1C2 for the expanded polyQ tracts (mouse monoclonal, 5TF1-1C2, 1:4000) (Millipore, Temecula, CA, USA), and A6RPT-#5803 for $Ca_v2.1$ C-terminal region (rabbit polyclonal, 1:500).[19] The primary antibodies were serially detected with the Vectastain ABC rabbit or mouse IgG kits (Vector Laboratories, Burlingame, CA, USA), and visualized by using Histofine Simple Stain DAB (Nichirei Bioscience, Tokyo, Japan) according to the manufacturer's protocol.

For double immunofluorescent labeling, sections were similarly treated as above and incubated with primary antibodies overnight at 4°C with anti-BDNF antibody (rabbit polyclonal, 1:50) (Santa Cruz Biotechnology) and 1C2 antibody (mouse monoclonal, 5TF1-1C2, 1:2000; Millipore). Sections were washed three times in PBS and incubated with fluoresecein-labeled anti-mouse IgG (heavy and light chains [H + L]) (1:250) (Vector Laboratories) and Alexa-fluor 555 goat anti-rabbit IgG (H + L) (1:250) (Invitorogen) for 1 h at room temperature. Sections were washed three times in PBS, incubated with 1% Sudan black B in 70% methanol for 5 min to reduce the autofluorescence, washed three times in PBS and incubated with 3% 4′,6-diamidino-2-phenylindole solution for 15 min at 37°C. Slides were observed under a confocal microscope (LSM 510META; Carl Zeiss, Jena, Germany).

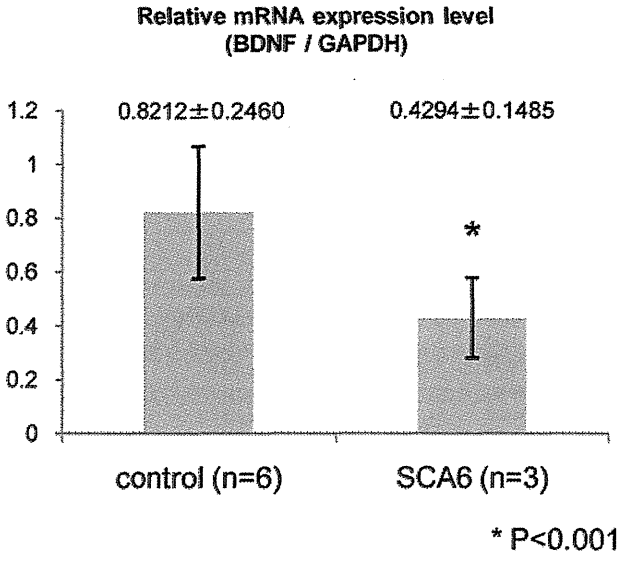

Fig. 1 Brain-derived neurotrophic factor (BDNF) expression level in spinocerebellar ataxia type 6 (SCA6) patients' cerebella is decreased in comparison with that in control patients' cerebella. Quantitative (q) RT-PCR reveals that the level of BDNF mRNA against that of glyceraldehyde 3-phosphate dehydrogenase (GAPDH) is significantly reduced in SCA6 cerebellum ($n = 3$) in comparison with controls ($n = 6$). (Control, ($n = 6$: 0.8212 ± 0.2460; SCA6, $n = 3$: 0.4294 ± 0.1485; $P = 0.0201$).

RESULTS

The *BDNF* mRNA expression level is decreased in SCA6 human cerebellum

The qRT-PCR analysis on each cDNA generated from SCA6 ($n = 3$) and control ($n = 6$) cerebellar tissues revealed that the level of *BDNF* mRNA against that of *GAPDH* mRNA was significantly reduced in SCA6 human cerebellum compared to controls (controls $n = 6$: 0.8212 ± 0.2460; SCA6, $n = 3$: 0.4294 ± 0.1485; $P = 0.0201$) (Fig. 1). This suggests that the *BDNF* mRNA expression level is decreased in SCA6 cerebellar cortex.

Observation of BDNF-immunoreactive granules in the dendrites of SCA6 Purkinje cells

To investigate whether there is a change for quantity and intracellular localization of BDNF protein in the SCA6 cerebellum, we undertook immunohistochemical analysis of SCA6 and control human cerebella with the anti-BDNF antibody. In control cerebellum, the BDNF-immunoreactivity was only weakly seen in all neurons, including the Purkinje cells and granule cells (Fig. 2a,b). The BDNF immunoreactivity was also quiescent in the SCA2 cerebellum (Fig. 2c), whereas 1C2-positive polyQ aggregates are seen in the Purkinje cell cytoplasm (Fig. 2d). In contrast, numerous BDNF-immunopositive granules were seen in the structures compatible with dendritic trees of SCA6 Purkinje cells (Fig. 2e,f, arrows). The BDNF granules were not conspicuous in the cell bodies (Fig. 2f, arrowhead) or axons of Purkinje cells. The antibody A6RPT-#5803 against the $Ca_v2.1$ C-terminus detected numerous $Ca_v2.1$ aggregates in the proximal dendrite (Fig. 2g, filled arrow) as well as in the cell body. Occasionally, they were present even in the distal part of the dendrites (Fig. 2g, open arrow), showing that the $Ca_v2.1$ aggregates exist in a wide range of dendritic arbors. The BDNF-positive structures similar to the ones seen in SCA6 Purkinje cells were sought in other areas of brains affected with polyQ diseases. However, we did not see any similar structures in as far as we investigated the cerebral cortex and the striatum of HD brains (Fig. 2h) and the pons of MJD patients. The present observation indicates that formation of BDNF-positive granules may be specific to SCA6 Purkinje cell dendrites.

BDNF-immunoreactive granules are observed in the vicinity of $Ca_v2.1$ aggregates

We next asked whether the presence of BDNF-immunoreactive granules is related to the formation of $Ca_v2.1$ aggregates known to be specific to SCA6 cell bodies and dendrites.[4,5,19] To address this question, we carried out a double immunofluorescence study against BDNF (red) and 1C2 (green).

We found that 1C2-positive polyQ aggregates often existed in the proximal portion of dendrites, such as the primary shaft (Fig. 3a, arrow) or the secondary shaft (Fig. 3b, arrow), of the Purkinje cells. On the other hand, the BDNF-immunoreactive structures were seen distal to the 1C2-positive polyQ aggregates (Fig. 3a,b). Curiously, we found that the BDNF-immunoreactive granules were seen not only within the contour of Purkinje cell dendrites (Fig. 3a,b), but also outside of the visible dendritic structures (Fig. 3c,d, arrowheads).

DISCUSSION

We made two fundamental observations in this study. One is the reduced *BDNF* mRNA level in the SCA6 cerebellum. The BDNF is a member of the neurotrophic family controlling many processes, including neurogenesis, proliferation, survival, synaptic transmission and activity-dependent synaptic plasticity.[11,13] The molecule is widely distributed in the CNS and is abundantly expressed in the cerebellar cortex, including Purkinje cells.[20] The BDNF appears to be involved in many polyQ diseases. In HD, reduced BDNF gene expression has been found in cultured cells,[14] an animal model,[15] and in patients' brains.[12,21] In addition, over-expression of BDNF gene in the striatum of

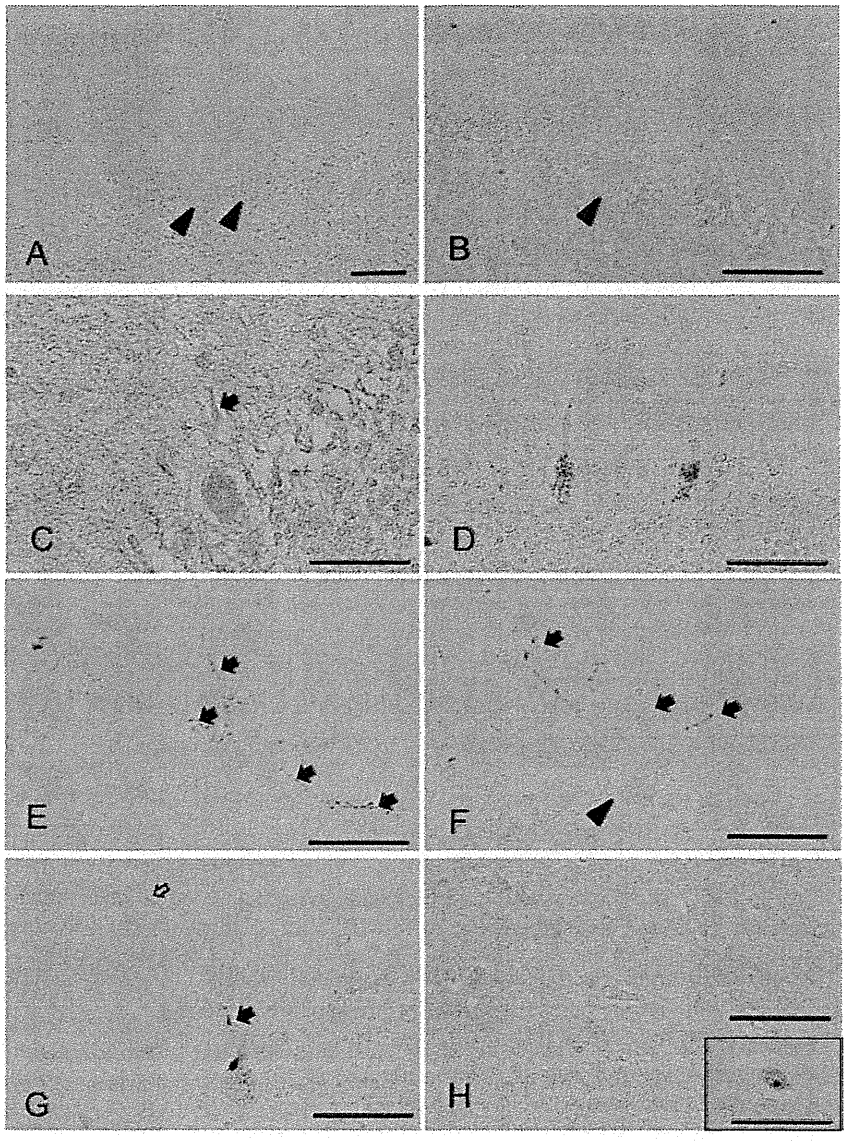

Fig. 2 Numerous brain-derived neurotrophic factor (BDNF)-immunoreactive granules are present in the dendrites of spinocerebellar ataxia type 6 (SCA6) Purkinje cells. (A, B) In control patients' cerebella, BDNF immunoreactivity is undetectable. Arrowheads indicate cell bodies of the Purkinje cells. (A, Parkinson's disease; B, SCA31). (C, D) In SCA2 cerebellum, BDNF immunoreactivity is also quiescent (C), but 1C2-positive granules are abundant in the Purkinje cell cytoplasm (D). (E, F) In a SCA6 Purkinje cell, numerous BDNF-immunoreactive granules are seen in the structures compatible with dendritic trees of Purkinje cells (arrows). BDNF granules are not conspicuous in the cell cytoplasm of Purkinje cells (arrowhead). (G) A6RPT-#5803 antibody, which is against α1A voltage-dependent calcium channel protein ($Ca_v2.1$) C-terminus, detects numerous $Ca_v2.1$ aggregates in the cell body of Purkinje cells and often in the proximal dendrite (filled arrow). $Ca_v2.1$ aggregates occasionally present even in the distal part of the dendrite (open arrow). (H) BDNF immunoreactivity is not seen in the striatum of Huntington's disease brains (large box), otherwise 1C2-positive aggregate are seen in the nuclei of striatal neurons (small box). (For A–G: scale bars; 50 μm).

HD mice compensates for reduced BDNF gene levels, ameliorating disease phenotypes.[15] The reduced BDNF gene expressions are also observed in a DRPLA cell model expressing mutant atrophin-1 and in SCA1 mouse models.[22,23] Interestingly, the drug 3,4-diaminopyridine improved motor behavior of mice by increasing BDNF expression levels.[23] These lines of evidence seem to indicate that BDNF has an important defence role in many polyQ diseases. The BDNF gene expression was also found to be reduced in affected areas of subjects with Alzheimer's disease[24] and Parkinson's disease,[25] suggesting that *BDNF* mRNA could be reduced in many neurodegenerative diseases. Considering that the BDNF is also abundantly expressed in Purkinje cells, it is possible to speculate that reduced BDNF gene expression in SCA6 cerebella may be related to the pathogenic mechanism of SCA6. However, the precise mechanism of BDNF mRNA reduction in SCA6 is not clear. While the presence of nuclear polyQ aggregates is causally associated with BDNF suppression in other polyQ diseases, such aggregates are extremely rare in SCA6 Purkinje cells.[5,19] Therefore, the mechanism reducing the BDNF gene expression in SCA6 may be different from other polyQ diseases. In cultured cell models, we recently found that the "cytoplasmic" $Ca_v2.1$ aggregates caused the reduction of CREB and phosphorylated(p)-CREB, the active CREB isoform, in the nuclei by sequestering them to the $Ca_v2.1$ aggregates in the cytoplasm (manuscript submitted). In SCA6 human brains, we also confirmed that CREB also co-localizes with $Ca_v2.1$ aggregates in Purkinje cell bodies. Thus, we speculate that the

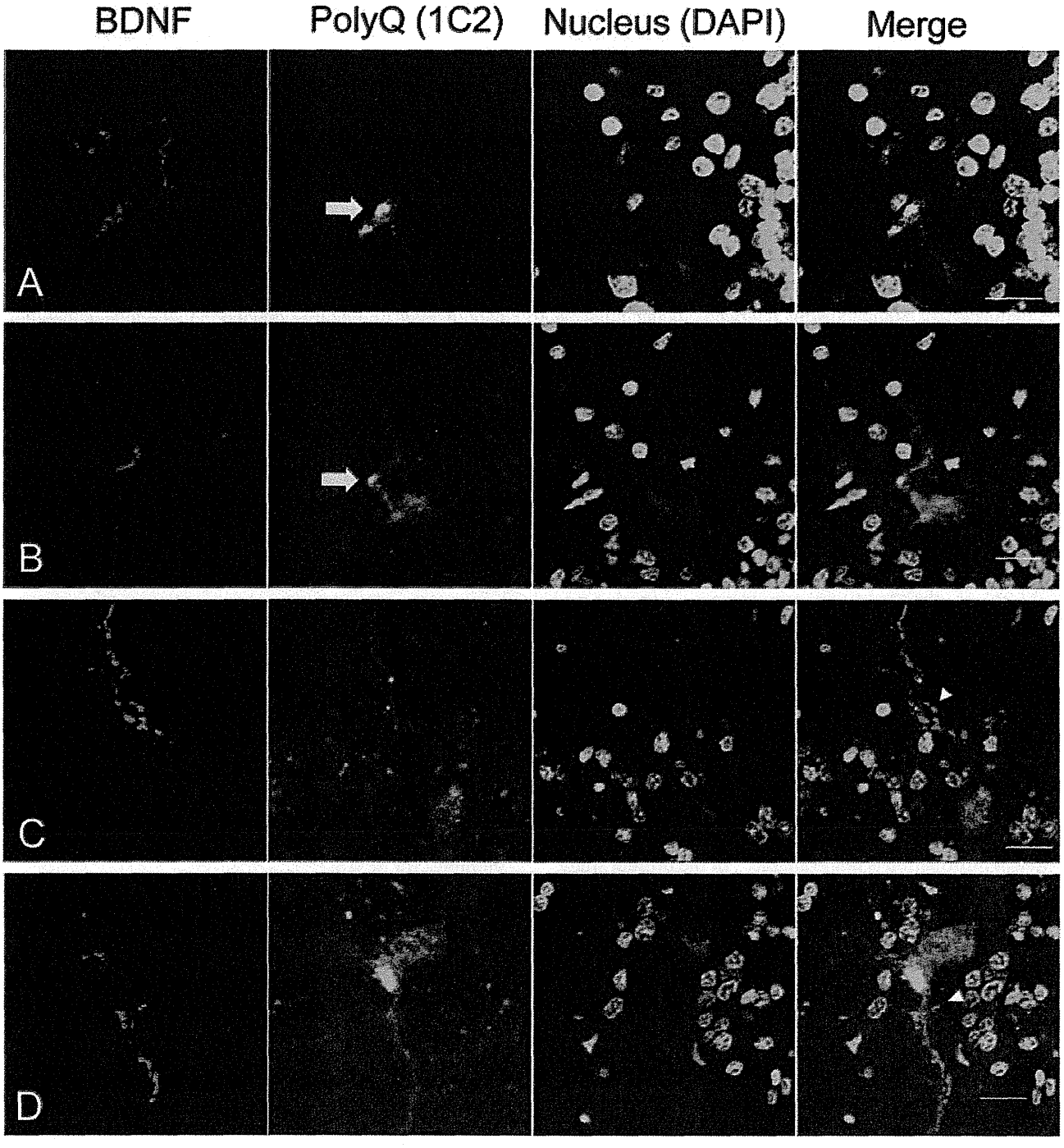

Fig. 3 The brain-derived neurotrophic factor (BDNF)-immunoreactive granules are observed in the vicinity of α1A voltage-dependent calcium channel protein ($Ca_v2.1$) aggregates. Double immunofluorescence with 1C2 antibody and anti-BDNF antibody in spinocerebellar ataxia type 6 (SCA6) patient cerebella. (A, B) 1C2-positive polyglutamine (polyQ) aggregates often existed in the proximal portion of dendrites, such as the primary shaft (A; arrow) or the secondary shaft (B; arrow), of Purkinje cells. BDNF-immunoreactive structures were seen distal to the 1C2-positive polyQ aggregates (A, B). (C, D) BDNF-immunoreactive granules were seen not only within the contour of Purkinje cell dendrites, but also outside the visible dendritic structures (arrow head). (For A–D: scale bars: 20 μm).

reduction of BDNF gene expression is due to reduced amounts of CREB in the nuclei by sequestration of CREB in the cytoplasm by $Ca_v2.1$ aggregates. Further studies are needed to elucidate how the cytoplasmic aggregates cause the suppression of CREB-target transcription.

The other key finding in the present study is that there are abundant BDNF-immunoreactive granules, mainly in the dendrites of SCA6 Purkinje cells. Previous studies indicate that these BDNF-immunoreactive granules are not stained by ubiquitin antibodies, since SCA6 lacks ubiquitin-positive structures.[4,26] As far as we have investigated in five SCA6 cerebellar specimens, the BDNF-immunoreactive granules were restricted to the Purkinje cells, similar to the $Ca_v2.1$ aggregates. For example, we did not observe any BDNF aggregates in the cerebellar granule cells or in the neurons of the dentate nucleus. Further studies using larger numbers of SCA6 patients would be important to address whether the BDNF granules are also seen in other SCA6 brain regions. Although we observed many BDNF-immunoreactive granules within dendrites under light microscopy, we also suspected that some of these granules appear to exist outside the dendritic contour. It may be possible that they are still inside the small dendritic sprouts, which were only invisible due to degeneration. Alternatively, they may have been secreted from the dendrites as previously postulated.[27] Precise investigation using electron microscopes is needed.

Previous studies investigating the BDNF immunohistochemistry in adult rat, guinea pig and Japanese macaque cerebella have shown that BDNF is expressed diffusely in the cell body and the dendrites of Purkinje cells.[20,28,29] One previous study describes granular BDNF immunoreactivity in the control human Purkinje cell dendrites, although detailed information is not available.[30] In the present study, we observed that BDNF immunoreactivity was very weak in human post mortem control specimens. This discrepancy in the immunostaining intensities between previous studies and the present one may be due to differences in tissue preparation, such as fixation: paraformaldehyde[12] or paraformaldehyde with picric acid[26] may be more suitable fixations for BDNF immunohistochemistry than the formalin we employed. Nevertheless, the granular BDNF-immunoreactive granules in Purkinje cells were specific to SCA6 in the present cohort, indicating that this finding is meaningful.

It is remains unclear how BDNF-immunoractive granules are formed in SCA6 Purkinje cells. The BDNF protein, still translated from reduced BDNF mRNA, needs to be subjected to many processes, such as post-translational modification and needs to be transported in cells to become functional. As we observed 1C2-immunoreactive $Ca_v2.1$ aggregates in the proximal portion of the dendrites, such as the primary shaft, it is tempting to speculate that BDNF trafficking in the dendrites may be disturbed, resulting in the formation of visible BDNF-immunoreactive granules in dendrites of SCA6 Purkinje cells. The $Ca_v2.1$ aggregates, shown by A6RPT-#5803 immunohistochemistry (Fig. 2g), were seen in the cell body through distal dendrites, suggesting that the $Ca_v2.1$ aggregates widely prevail in the somato-dendritic cytoplasm. The BDNF normally moves in the dendrites in both directions (antero- and retro-grade transports) between the post-synaptic button and cell body,[31] as well as from the cell body to the presynaptic terminal through anterograde axonal transport. Therefore, it may be possible that $Ca_v2.1$ aggregates disturbed BDNF trafficking in the dendrites. Interestingly, SCA2, which also forms polyQ aggregates in the cytoplasm of Purkinje cells (Fig. 2c), did not show similar BDNF-immunoreactive granules in the dendrites of Purkinje cells. Therefore, it may be possible that a certain factor specific to $Ca_v2.1$ may underlie formation of BDNF-positive granules. For example, the secretion of BDNF from dendrites (post-synaptic secretion) is considered regulated by intracellular Ca^{2+} concentration, which is in turn regulated by *N*-methyl-D-aspartate receptors, inositol tri-phosphate receptor (IP3R) and voltage-dependent calcium channels including $Ca_v2.1$.[32] Further studies are needed to address how $Ca_v2.1$ formation leads to BDNF-immunoreactive granules in the dendrites.

In conclusion, the decrease of BDNF gene expression level and abnormal BDNF-immunoreactive granules were seen in SCA6 cerebellum. Precise understanding of the implication of altered gene expressions, including BDNF, and of the mechanism generating BDNF-immunoreactive granules, may be important for establishing fundamental therapies for SCA6.

ACKNOWLEDGMENTS

This study was funded by the Japanese Ministry of Education, Sports and Culture (KI and HM), the Japan Society for Promotion of Science (JSPS) (KI and HM), the 21st Century COE Program on Brain Integration and its Disorders from the Japanese Ministry of Education, Science and Culture (HM), the Strategic Research Program for Brain Sciences by the Ministry of Education, Culture, Sports, Science and Technology of Japan (HM), Core Research for Evolutional Science and Technology (CREST), Japan Science and Technology Agency (JST), Saitama, Japan (HM), from the Health and Labour Sciences Research Grants on Ataxic Diseases (HM) of the Japanese Ministry of Health, Labour and Welfare, Japan, and by a Grant-in-Aid for Scientific Research on Innovative Areas (Comprehensive Brain Science Network) from the Ministry of Education, Science, Sports and Culture of Japan (SM).

The authors thank Mr. Noboru Ando and Mrs. Hitomi Matsuo (Tokyo Medical and Dental University) for their excellent technical assistance.

AUTHOR CONTRIBUTIONS

M. Takahashi, the first author, performed research, analyzed data and wrote the manuscript, while four others (NS, MO, YN and TI) partly performed research, and seven others (MY, HT, TK, OM, M. Takao, SM and YE) performed neuropathological examinations and assisted pathological analysis of this study, HM organized and arranged the whole project and KI designed, directed and wrote this work.

REFERENCES

1. Ishikawa K, Tanaka H, Saito M *et al.* Japanese families with autosomal dominant pure cerebellar ataxia map to chromosome 19p13.1-p13.2 and are strongly associated with mild CAG expansions in the spinocerebellar ataxia type 6 gene in chromosome 19p13.1. *Am J Hum Genet* 1997; **61**: 336–346.
2. Gomez CM, Thompson RM, Gammack JT *et al.* Spinocerebellar ataxia type 6: gaze-evoked and vertical nystagmus, Purkinje cell degeneration, and variable age of onset. *Ann Neurol* 1997; **42**: 933–950.
3. Zhuchenko O, Bailey J, Bonnen P *et al.* Autosomal dominant cerebellar ataxia (SCA6) associated with small polyglutamine expansions in the alpha 1A-voltage-dependent calcium channel. *Nat Genet* 1997; **15**: 62–69.
4. Ishikawa K, Fujigasaki H, Saegusa H *et al.* Abundant expression and cytoplasmic aggregations of [alpha]1A voltage-dependent calcium channel protein associated with neurodegeneration in spinocerebellar ataxia type 6. *Hum Mol Genet* 1999; **8**: 1185–1193.
5. Ishikawa K, Owada K, Ishida K *et al.* Cytoplasmic and nuclear polyglutamine aggregates in SCA6 Purkinje cells. *Neurology* 2001; **56**: 1753–1756.
6. Yabe I, Sasaki H, Matsuura T *et al.* SCA6 mutation analysis in a large cohort of the Japanese patients with late-onset pure cerebellar ataxia. *J Neurol Sci* 1998; **156**: 89–95.
7. Takahashi H, Ishikawa K, Tsutsumi T *et al.* A clinical and genetic study in a large cohort of patients with spinocerebellar ataxia type 6. *J Hum Genet* 2004; **49**: 256–264.
8. Orr HT, Zoghbi HY. Trinucleotide repeat disorders. *Annu Rev Neurosci* 2007; **30**: 575–621.
9. DiFiglia M, Sapp E, Chase KO *et al.* Aggregation of huntingtin in neuronal intranuclear inclusions and dystrophic neurites in brain. *Science* 1997; **277**: 1990–1993.
10. Paulson HL, Perez MK, Trottier Y *et al.* Intranuclear inclusions of expanded polyglutamine protein in spinocerebellar ataxia type 3. *Neuron* 1997; **19**: 333–344.
11. Binder DK, Scharfman HE. Brain-derived neurotrophic factor. *Growth Factors* 2004; **22**: 123–131.
12. Ferrer I, Goutan E, Marin C, Rey MJ, Ribalta T. Brain-derived neurotrophic factor in Huntington disease. *Brain Res* 2000; **866**: 257–261.
13. Zuccato C, Cattaneo E. Role of brain-derived neurotrophic factor in Huntington's disease. *Prog Neurobiol* 2007; **81**: 294–330.
14. Zuccato C, Ciammola A, Rigamonti D *et al.* Loss of huntingtin-mediated BDNF gene transcription in Huntington's disease. *Science* 2001; **293**: 493–498.
15. Gharami K, Xie Y, An JJ, Tonegawa S, Xu B. Brain-derived neurotrophic factor over-expression in the forebrain ameliorates Huntington's disease phenotypes in mice. *J Neurochem* 2008; **105**: 369–379.
16. Steffan JS, Kazantsev A, Spasic-Boskovic O *et al.* The Huntington's disease protein interacts with p53 and CREB-binding protein and represses transcription. *Proc Natl Acad Sci USA* 2000; **97**: 6763–6768.
17. Nucifora FC, Jr, Sasaki M, Peters MF *et al.* Interference by huntingtin and atrophin-1 with cbp-mediated transcription leading to cellular toxicity. *Science* 2001; **291**: 2423–2428.
18. McCampbell A, Taylor JP, Taye AA *et al.* CREB-binding protein sequestration by expanded polyglutamine. *Hum Mol Genet* 2000; **9**: 2197–2202.
19. Ishiguro T, Ishikawa K, Takahashi M *et al.* The carboxy-terminal fragment of alpha(1A) calcium channel preferentially aggregates in the cytoplasm of human spinocerebellar ataxia type 6 Purkinje cells. *Acta Neuropathol* 2010; **119**: 447–464.
20. Dieni S, Rees S. Distribution of brain-derived neurotrophic factor and TrkB receptor proteins in the fetal and postnatal hippocampus and cerebellum of the guinea pig. *J Comp Neurol* 2002; **454**: 229–240.
21. Gauthier LR, Charrin BC, Borrell-Pages M *et al.* Huntingtin controls neurotrophic support and survival of neurons by enhancing BDNF vesicular transport along microtubules. *Cell* 2004; **118**: 127–138.
22. Miyashita T, Tabuchi A, Fukuchi M *et al.* Interference with activity-dependent transcriptional activation of BDNF gene depending upon the expanded polyglutamines in neurons. *Biochem Biophys Res Commun* 2005; **333**: 1241–1248.
23. Hourez R, Servais L, Orduz D *et al.* Aminopyridines correct early dysfunction and delay neurodegeneration in a mouse model of spinocerebellar ataxia type 1. *J Neurosci* 2011; **31**: 11795–11807.